Supporting Information

Synthesis and Intramolecular Singlet Fission Properties of *Ortho*-Phenylene Linked Oligomers of Diphenylhexatriene

Oliver Millington[ab], Ashish Sharma[b], Stephanie Montanaro[a], Anastasia Leventis[a], Simon A. Dowland[b], Daniel G. Congrave[a], Cherie-Anne Lee[a], Akshay Rao*[b], Hugo Bronstein*[ab]

a Department of Chemistry, University of Cambridge, Cambridge, CB2 1EW, UK.
b Cavendish Laboratory, University of Cambridge, Cambridge, CB3 0HE, UK.

Table of Contents

1. General Experimental Details

All general experimental details for synthesis, synthetic characterisation, transient absorption spectroscopy, time-correlated single photon counting, photoluminescence quantum yield, steady-state absorption and steady-state photoluminescence were as reported in detail in the supplementary information of our previous work.[1]

2. Steady-State Absorption and Photoluminescence Spectra

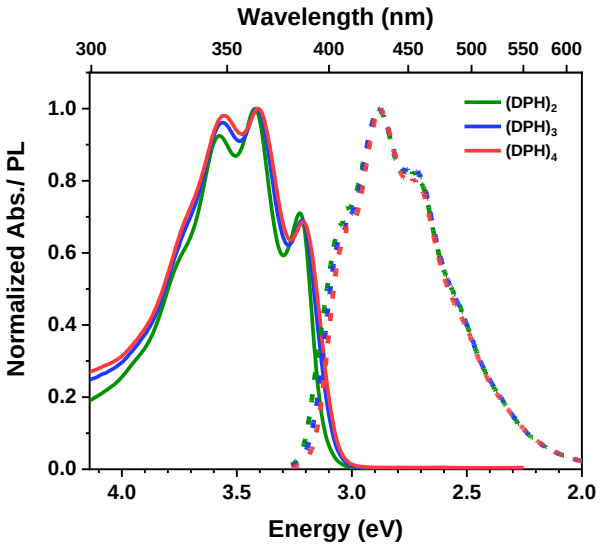

Figure S1. UV–Vis absorption (solid line) and photoluminescence (dashed line) spectra of dilute solutions (~5 to 10 μM) in toluene. Photoluminescence spectra were recorded with excitation at 355 nm.

3. Further Transient Absorption Spectroscopy

i) fsTA: Spectral Evolution of The Triplet-Pair State

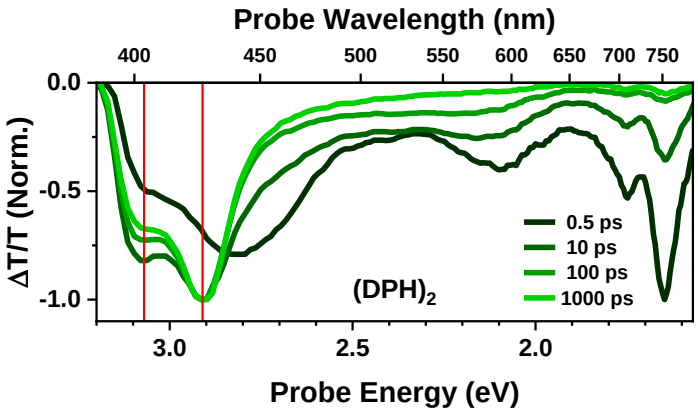

Figure S2. fsTA spectra of 1 mM $(DPH)_2$, normalized to the PIA maximum. The red-lines at 3.07 eV and 2.91 eV emphasize the centres of the main peak and high energy shoulder in the triplet-pair PIA. This shoulder diminishes in relative intensity over time but does not arise from the singlet itself (indicated by the 0.5 ps spectrum). This high energy shoulder may indicate that there is a binding energy associated with the initially formed ^{1}(TT) state. Logically if the ^{1}(TT) energy is reduced relative to weakly interacting triplets by a binding energy, then this can be anticipated to result in an increase in the energy of the $T_1 \rightarrow T_n$ transition.

ii) fsTA: Spectra Across the Concentration Ranges

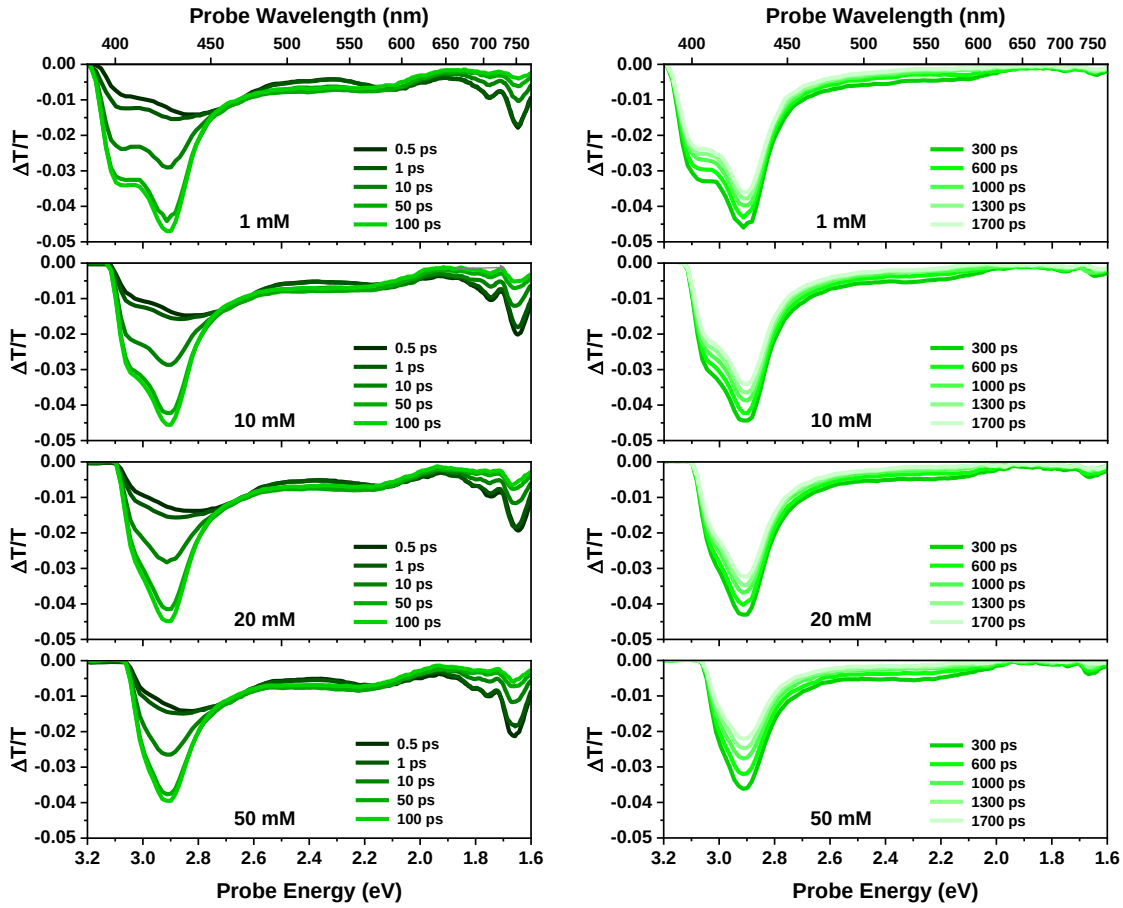

Figure S3. fsTA spectra of $(DPH)_2$ at the different concentrations that were measured, showing time intervals up to the peak of the TT PIA signal (left) and late time intervals in which the TT PIA decays (right).

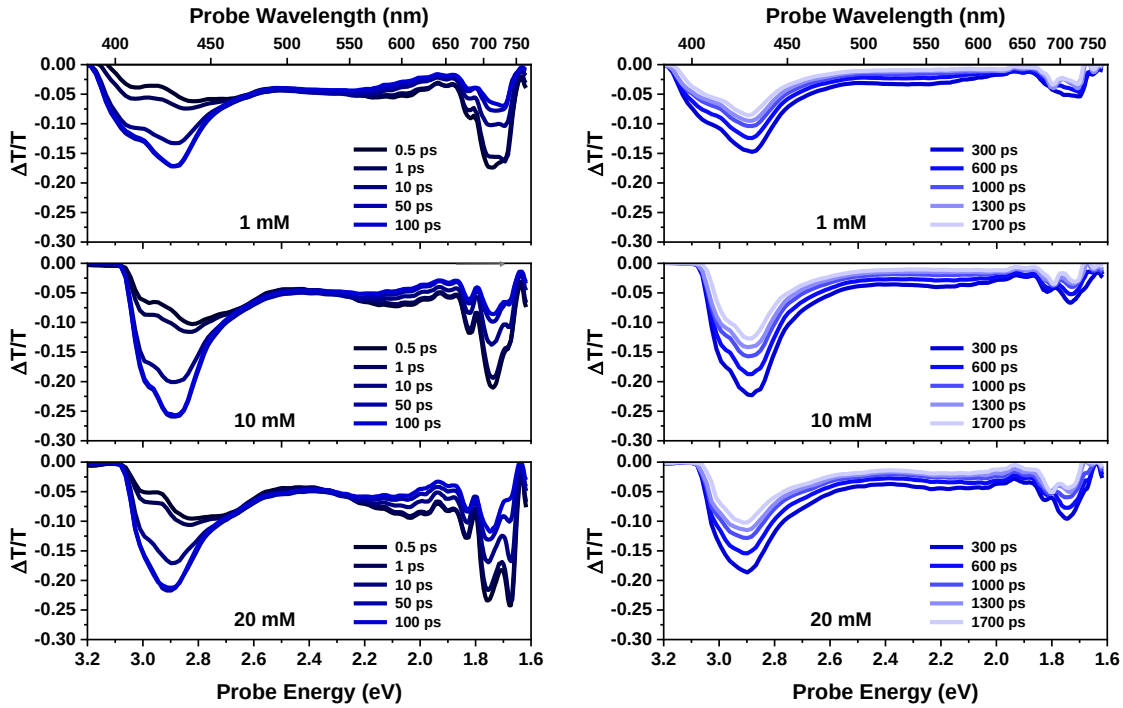

Figure S4. fsTA spectra of $(DPH)_3$ at the different concentrations that were measured, showing time intervals up to the peak of the TT PIA signal (left) and late time intervals in which the TT PIA decays (right).

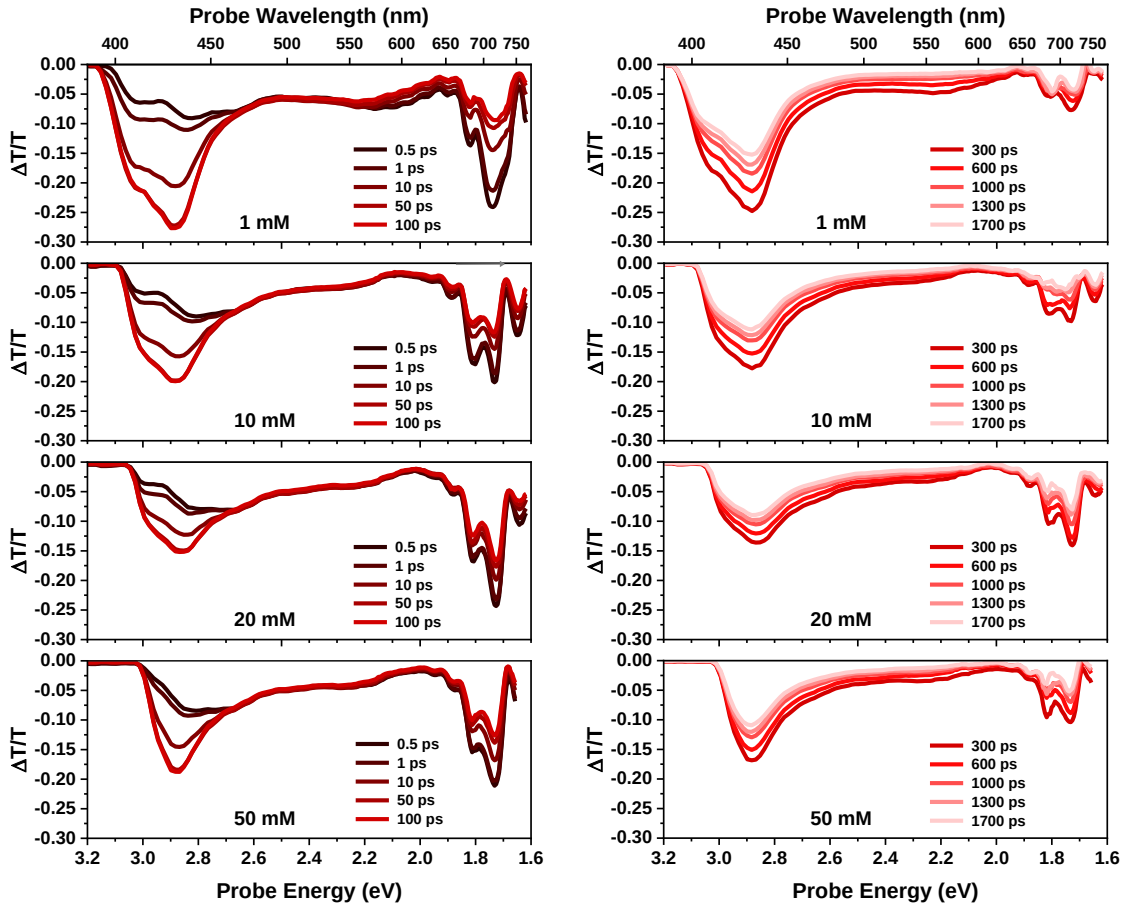

Figure S5. fsTA spectra of $(DPH)_4$ at the different concentrations that were measured, showing time intervals up to the peak of the TT PIA signal (left) and late time intervals in which the TT PIA decays (right).

ii) nsTA: Contour plots, Comparison to Sensitization, and Kinetics

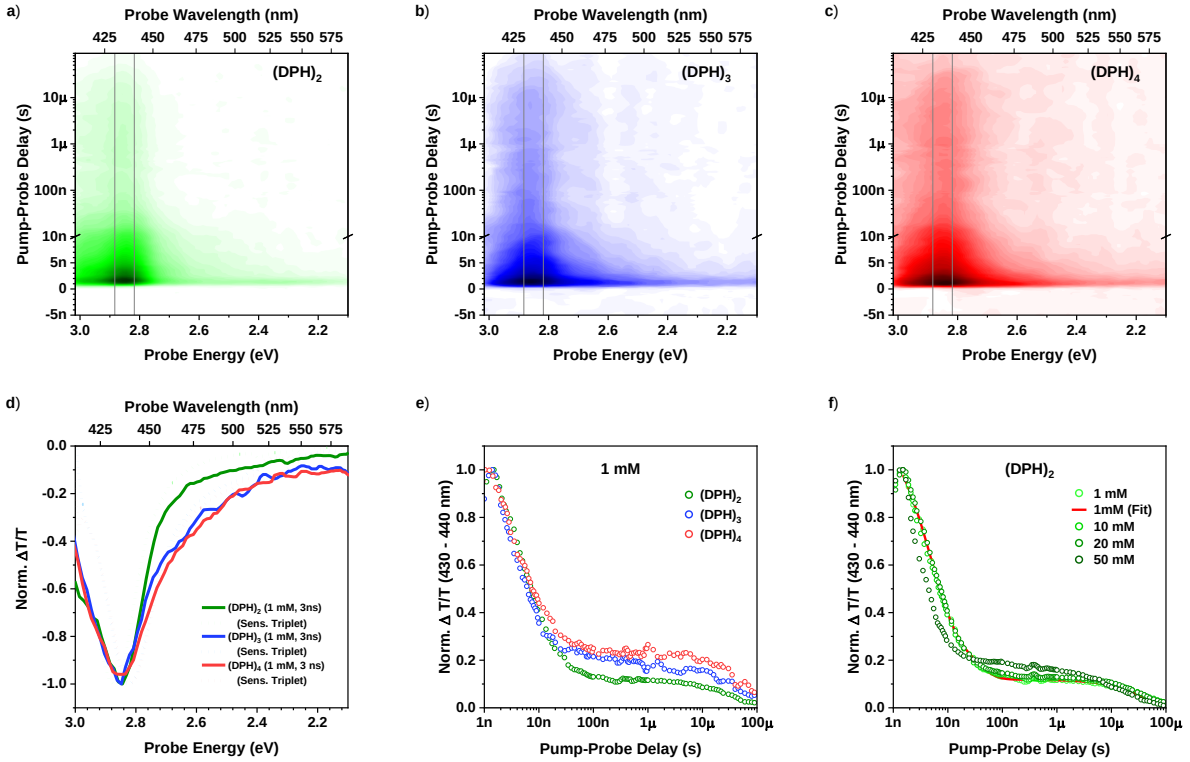

Figure S6. a)-c) nsTA contour plots of $(DPH)_2$, $(DPH)_3$ and $(DPH)_4$ with excitation at 355 nm. The data shown are for 1 mM but are representative of all studied concentrations which varied little. d) Comparison of the dilute nsTA spectra of the neat oligomer solutions, taken as a spectral slice at the early pump-probe delay interval of 3 ns, to the triplet spectra produced by sensitization with PdOEP. Sensitization experiments were carried out in mixed solutions of PdOEP (120 µM) and oligomer (5 mM), selectively exciting the sensitizer with a 532 nm pump beam. The sensitized triplet spectra shown are spectra averaged over late time intervals (500 ns – 10 µs), after decay of the PdOEP ground state bleach was completed indicating that complete triplet transfer had occurred. Under these measurement conditions the (sensitized) triplet lifetimes of $(DPH)_2$, $(DPH)_3$ and $(DPH)_4$ were determined to be 47.1±0.9 µs, 50±1 µs and 49±1 µs respectively. e) Kinetics in the region of the triplet peak (430-440 nm), which is between the grey lines indicated on the contour plots, for 1 mM solutions of each material. f) Kinetics as in (e) but for the $(DPH)_2$ concentration series. A triexponential fit is also plotted for the 1mM case. The fit parameters are: $\tau_1 = 4.5$ ns $(A_1 = 0.68)$,: $\tau_2 = 25.6$ ns $(A_1 = 0.22)$,: $\tau_3 = 40$ µs $(A_1 = 0.10)$. The major lifetime component, τ_1, can be taken as the triplet-pair annihilation timescale that harvesting schemes would need to outcompete.

4. Estimation of Collisional Timescales as a Function of Concentration

The frequency of collisions of molecules in solution is governed by the process of diffusion. On a fundamental level, diffusion is the result of Brownian motion;[2] before any two initially separated solute molecules collide, each will experience very many collisions with the surrounding solvent that change the speed and direction of the solute.

i) Collision Theory Model

The Basis: Smoluchowski Model for Spherical reactants

The classical model that can be applied to describe the diffusive bimolecular collision rate is the Smoluchowski limit for two spherical molecules A and B:[3]

$$Z\ (s^{-1}m^{-3}) = 4\pi(R_A + R_B)(D_A + D_B)C_A C_B$$

- Where Z is the collision frequency in number of collisions per second per unit volume (1 m^3).
- R_A and R_B are the radii of molecules A and B respectively.
- D_A and D_B are the diffusion constants of A and B respectively, which can be determined using diffusion order nuclear paramagnetic resonance spectroscopy (DOSY NMR).
- C_A and C_B are the concentrations of A and B in number of particles per unit volume (m^3).

For the consideration of a collision between like molecules, A = B so we may simplify the expression and drop the subscript in D and C:

$$Z(s^{-1}m^{-3}) = 16\pi RDC^2$$

However, we are particularly interested in the collisional timescale and must accordingly convert the number of collisions per unit volume per unit time to the number of collisions per particle per unit time by dividing by the number of particles per unit volume (i.e. C):

$$Z(s^{-1}) = 16\pi RDC$$

We may also convert the concentration from units of m^{-3} to molar units, 1M = 1000 mol m^{-3}, using Avogadro's constant, N_A:

$$C_{(m^{-3})} = 1000N_A \times C_{(M)}$$

$$Z(s^{-1}) = 16000\pi N_A RDC_{(M)}$$

The collisional timescale is then given by the reciprocal of the collision rate per particle:

$$\tau\,(\mathrm{s}) = \frac{1}{Z}$$

Determination of effective values for molecular radii, R*

Unfortunately, collision of the DPH oligomers discussed in this work would be poorly approximated by treating the molecules as spheres with a radius R that may interact in any orientation. The matter of collisions of non-spherical molecules is complex and the reader may reflect upon the following quotation from a relevant review by Berg and Von Hippel:[4]

"3.2.3 ARBITRARY GEOMETRIES For arbitrary geometries of the molecules and their reactive regions, a detailed derivation of the effects of orientational constraints becomes impossible."

It is however possible to generate an effective radius, R*, for non-spherical molecules with simple geometries.[4] A rod like molecule may be approximated by an ellipsoid with major and minor semi-axes of *a* and *b* respectively**.** In this case: [4]

$$R^* \simeq \frac{a}{\ln\left(\frac{2a}{b}\right)}$$

As a first example, the DPH chromophore can be modelled as such a linear rod (Figure S7). So, for the DPH monomer R* could be determined:

$$R^*_{DPH} \simeq \frac{14 \times 10^{-10}}{2 \times \ln\left(\frac{14}{(3/2)}\right)} = 3 \times 10^{-10}\ \mathrm{m}$$

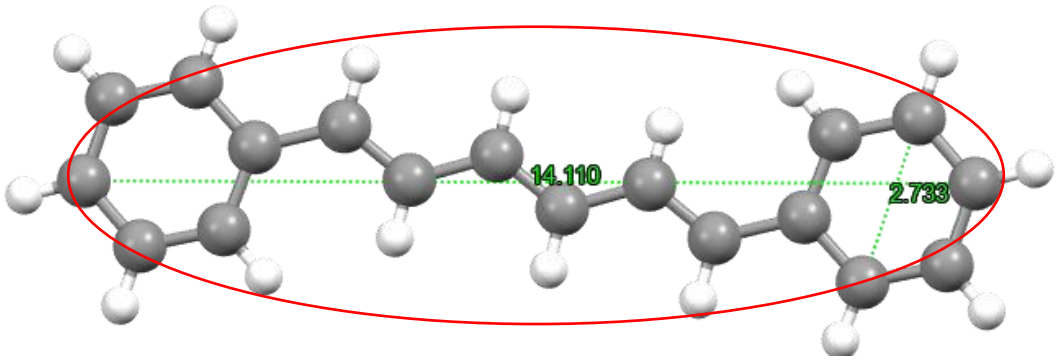

Figure S7. The structure of DPH utilizing crystal structure data from Harada *et al.*[5] The measured distanced (Angstroms) may be applied as major and minor axes in a "rod" model to determine the effective reactive surface area for collisions involving DPH (2*a* = 14.11 Å ~ 14 Å, 2b = 2.73 Å ~ 3 Å). The red oval (2D projection of an ellipsoid) has no mathematical meaning but is placed to guide the reader in seeing the approximation of DPH with an ellipsoid.

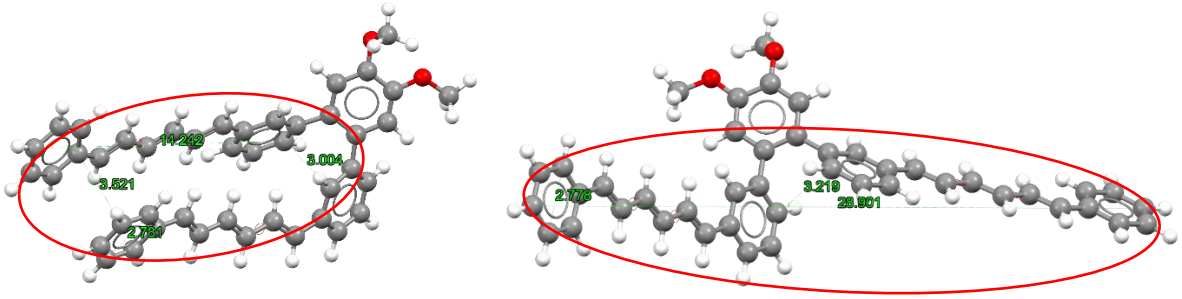

Figure S8. Computationally optimized conformer geometries of $(DPH)_2$. Optimization was carried out in the ground state using the Gaussian 16 DFT software.[6] The M06-2X functional,[7] was utilized together with the def2-SVP basis set.[8] As in Figure S7 the red-ovals are placed to guide the eye.

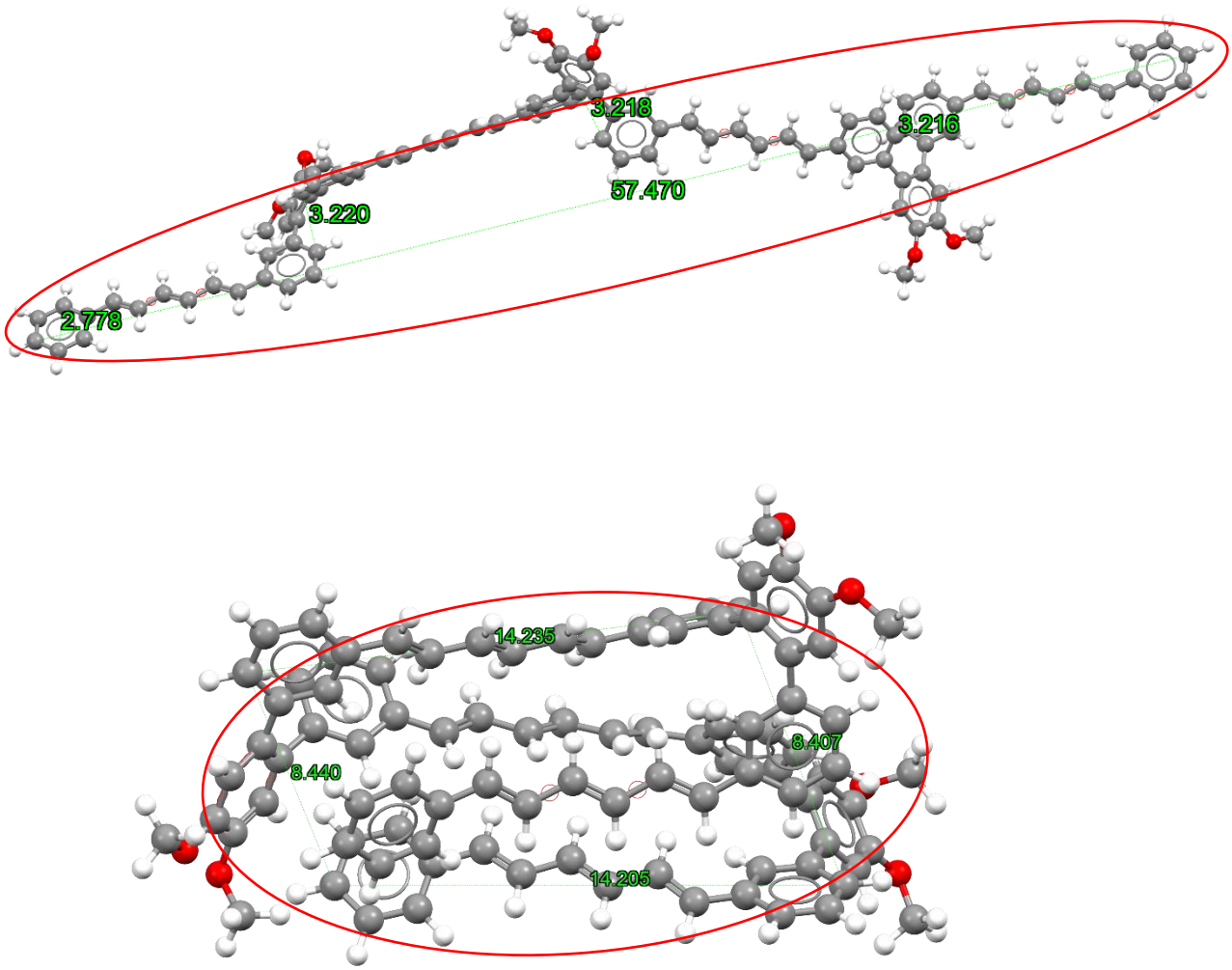

Figure S9. Computationally optimized conformer geometries of $(DPH)_4$. The extreme cases of fully "folded" and fully "unfolded" geometries have been calculated. Red ovals are placed to guide the eye.

We may now consider the possible geometry of the dimer $(DPH)_2$ (Figure S8). The dimer geometry was optimized computationally using density functional theory (DFT). We note that molecules such as the oligomers may be expected to exhibit multiple different stable geometries (conformers) corresponding to local minima in the potential energy surface. Optimization by DFT can be expected to find the nearest local energy minimum (conformer). Starting with different initial guess geometries two conformer geometries were optimized by DFT for $(DPH)_2$. In one conformer the DPH units are "folded" over each other in a cofacial arrangement. In the other, the dimer has been "unfolded". In either case the calculated length scales for each DPH chromophore unit are consistent with those determined from the crystal structure data of Harada *et al.* We can make a rough approximation of the shape of each conformer using the ellipsoid model. This will be less "good" a model than for the simple monomer but should be sufficient to demonstrate the approximate effective size of the molecule for collisions. In the cofacial geometry, the major axis is evidently the same as that of the DPH monomer. Additionally, the cofacial separation is of similar magnitude (~ 3.5 Å) as the "width" of each DPH unit. Effectively, the cofacial geometry does not significantly increase the "capture radius" of the molecule relative to DPH monomer. However, in the unfolded geometry if the overall structure is modelled again as an ellipsoid rod, then the major axis is increased to ~ 29 Å, altering the R* value.

$$\text{Folded: } R^*_{(DPH)_2} \simeq \frac{14 \times 10^{-10}}{2 \times \ln\left(\frac{14}{(3/2)}\right)} = 3 \times 10^{-10} \text{ m}$$

$$\text{Unfolded: } R^*_{(DPH)_2} \simeq \frac{29 \times 10^{-10}}{2 \times \ln\left(\frac{29}{(3/2)}\right)} = 5 \times 10^{-10} \text{ m}$$

A similar approach can be applied to the tetramer (Figure S9):

$$\text{Unfolded: } R^*_{(DPH)_4} \simeq \frac{57 \times 10^{-10}}{2 \times \ln\left(\frac{57}{(3/2)}\right)} = 8 \times 10^{-10} \text{ m}$$

$$\text{Folded: } R^*_{(DPH)_4} \simeq \frac{14 \times 10^{-10}}{2 \times \ln\left(\frac{14}{(8/2)}\right)} = 6 \times 10^{-10} \text{ m}$$

Ultimately the point of this exercise has been to demonstrate that even conformers at opposite extremes of "foldedness" result in capture radii that are similar in magnitude. Furthermore, assuming that the geometry of each oligomer is approximately evenly distributed across the possible conformers then we can take forward an average value of R* for each oligomer:

$$R^*_{(DPH)_2} \sim 4 \times 10^{-10} \text{ m}$$

$$R^*_{(DPH)_4} \sim 7 \times 10^{-10} \text{ m}$$

ii) DOSY NMR of $(DPH)_2$ and $(DPH)_4$

Diffusion ordered nuclear magnetic resonance spectroscopy (DOSY) was carried out on the limiting case oligomers, $(DPH)_2$ and $(DPH)_4$, in order to determine the diffusion coefficients, D:

$(DPH)_2$: $D = 4.7 \times 10^{-10} m^2 s^{-1}$

$(DPH)_4$: $D = 2.9 \times 10^{-10} m^2 s^{-1}$

We note that these values are of the same order of magnitude as that reported for the similarly sized pentacene-tetracene dimer PT2 ($D = 6.8 \times 10^{-10} m^2 s^{-1}$).[9]

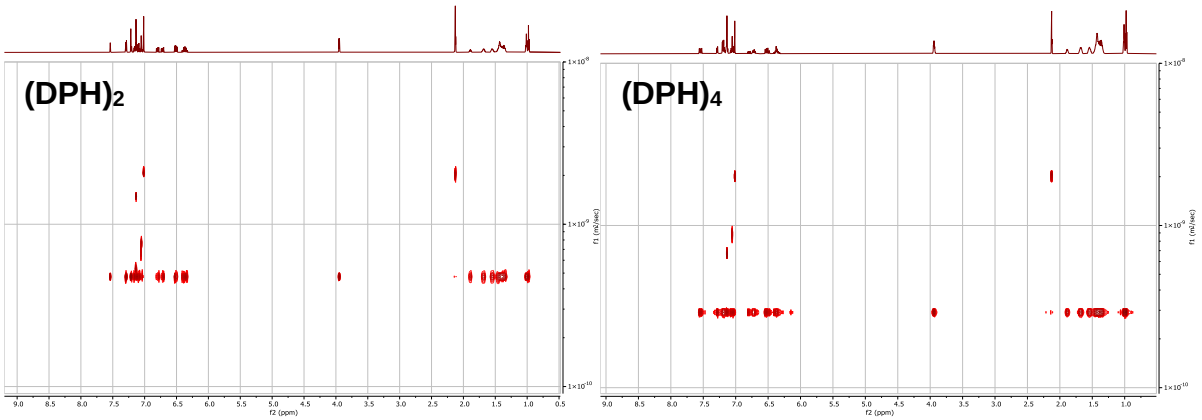

Figure S10. DOSY NMR spectra of d_8-toluene solutions (~10 mM) of $(DPH)_2$ and $(DPH)_4$. Residual solvent signals are visible at 7.14, 7.06, 7.01 and 2.13 ppm. There is some dispersion of the solvent signals in the D axis. This suggests that the solute molecules have a non-negligible impact on the local viscosity in their immediate environment.

iii) Equations for the collisional timescale as a function of concentration

To the first order approximation, using the above results for R and D we can generate the mean collision timescale as a function of concentration for each material:

$$\tau\,(\mathrm{s}) = \frac{1}{16000\pi N_A R D C_{(M)}}$$

$$\tau_{(DPH)_2}\,(\mathrm{s}) \sim \frac{1}{16000\pi N_A (4\times10^{-10})(4.7\times10^{-10})}\,\frac{1}{C_{(M)}} \sim \frac{1.7\times10^{-10}}{C_{(M)}}$$

$$\tau_{(DPH)_4}\,(\mathrm{s}) \sim \frac{1}{16000\pi N_A (7\times10^{-10})(2.9\times10^{-10})}\,\frac{1}{C_{(M)}} \sim \frac{1.6\times10^{-10}}{C_{(M)}}$$

It is clear that the gradients of these two lines are virtually identical (Figure S11). This arises due to the inverse relationship that diffusivity has with molecular size.[10] For ideal spherical molecules the product RD would be constant, and the lines would superimpose exactly.

Let us define the critical concentration, C_{Crit}, as the concentration at which $\tau_{Collisions} = \tau_{TT}$. We see from Figure S11 that C_{Crit} ~ 40 mM. We may estimate the magnitude of the effect of collisional harvesting at C_{crit} if collisions are indeed successful at separating the triplet pair:

i) The triplet-pair population decays exponentially: $\frac{n}{n_0} = e^{-\frac{t}{\tau_{TT}}}$

ii) At t = τ_{TT}: $\frac{n}{n_0} = e^{-1} = 0.37$

iii) 0.37 is the proportion of triplet pairs that can be harvested within the mean collisional timescale. If harvesting was efficient, then the population of long-lived molecularly isolated triplets would increase by 0.37 of the peak triplet-pair population.

At 50 mM, which is greater than C_{crit}, we see no such significant increase in the ratio of long-lived triplet states to the triplet pair peak (figure S6.e), indicating that collisional harvesting is ineffective for $(DPH)_2$. The same result is observed in the larger oligomers.

It is important to note that the onset of concentration effects would be anticipated to occur significantly below the critical concentration, since some collisions will occur faster than the mean timescale. If the onset of noticeable effects was to occur at an order of magnitude lower than the critical concentration, then this would correspond to a threshold concentration of ~ 4mM. This is remarkably consistent with the experimental onset determined for observation of intermolecular singlet fission in solutions of monomeric singlet fission materials.[1,11,12]

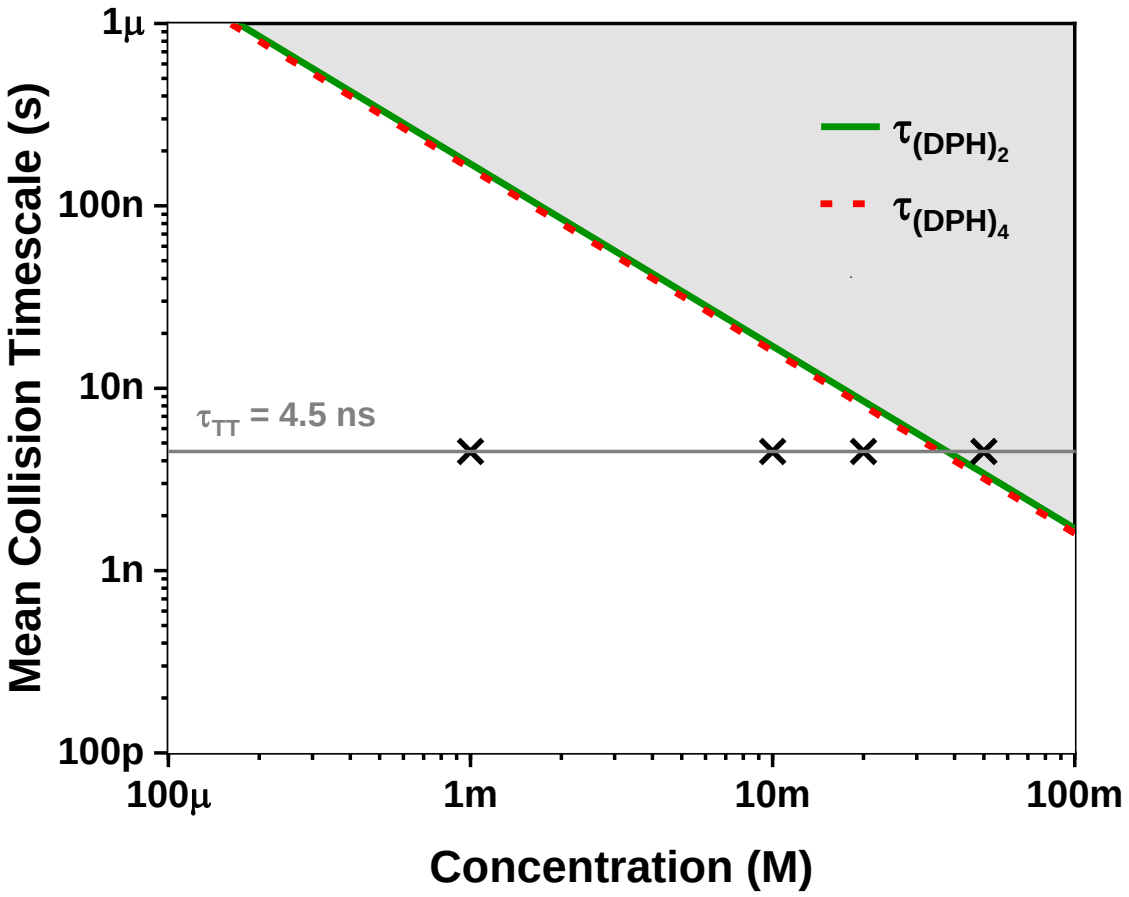

Figure S11. Plot of the collision timescale versus concentration for $(DPH)_2$ and $(DPH)_4$. The oligomer size does not significantly alter the dependence of the collision rate on the concentration. The triplet-pair annihilation lifetime of 4.5 ns (see fit in Figure S6.f.) is indicated, and upon this line crosses note the concentration series studied for $(DPH)_2$ in this work.

5. Fluorescence Lifetimes and Yields

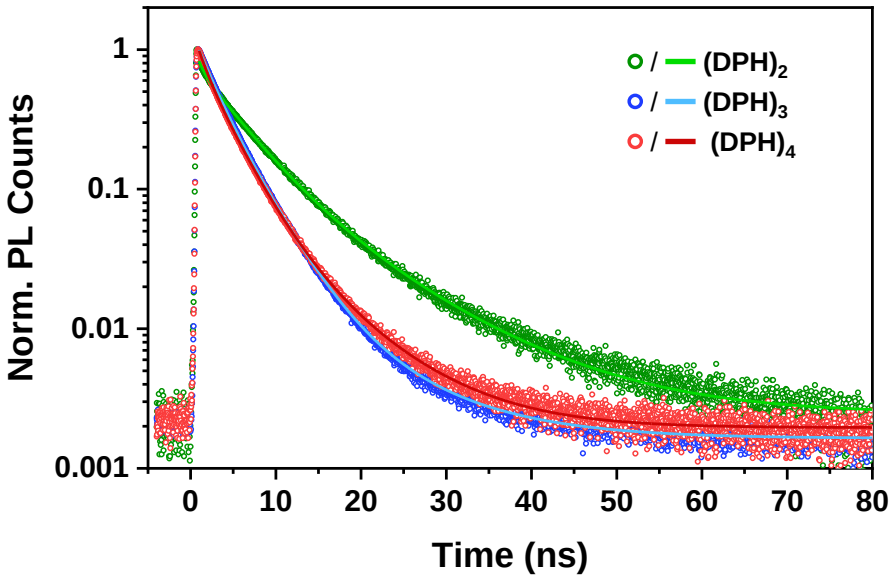

Figure S9. Time-correlated single photon counting emission lifetime plot of 100 µM solutions excited at 375 nm. Symbols represent the raw data, while lines indicate the fits to the data. Fits are the result of the minimum number of exponential terms required to accurately describe each decay (which in all cases is three) with the corresponding parameters indicated in Table S1.

Table S1. Fluorescence yields and lifetimes (100 µM)

Compound	PLQE / %	$\tau(\tau_1; \tau_2; \tau_3)$ / ns	Relative Amplitudes ($A_1; A_2; A_3$)
$(DPH)_2$	15	1.3; 5.5; 17.1	0.33; 0.63; 0.04
$(DPH)_3$	16	1.8; 3.7; 10.2	0.34; 0.64; 0.02
$(DPH)_4$	13	1.1; 3.3; 8.2	0.31; 0.63; 0.06

6. Syntheses

i) Synthesis of a Dialkoxy Substituted Phenylene Linker [2]

Scheme S1

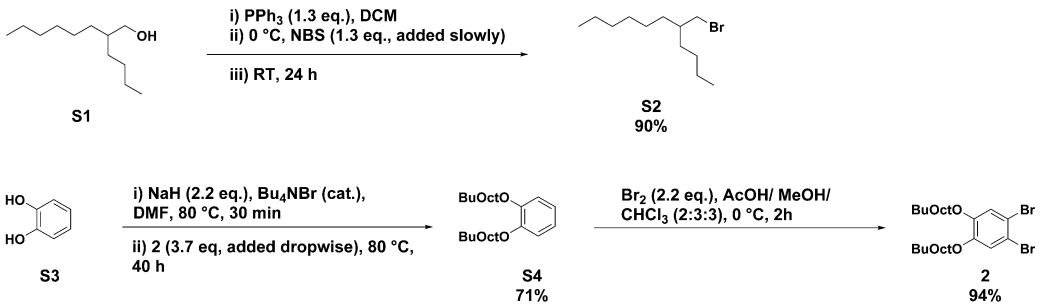

5-(bromomethyl)undecane [S2]

2-butyloctanol, **S1**, (81 mL, 360 mmol, 1.0 eq.), was added to a dry round bottom flask and DCM (180 mL) added. Triphenylphosphine (104 g, 396 mmol, 1.3 eq.) was added in one portion and the reaction cooled to 0 °C. N-bromosuccinimide (70 g, 393 mmol, 1.3 eq.) was added slowly over the course of 30 minutes. The reaction mixture was allowed to warm to room temperature and stirred for 24 hours. The reaction mixture was filtered through celite to remove solid triphenylphosphine oxide by-product and the filtrate was concentrated *in vacuo.* The crude product was triturated in hexane and filtered through celite then concentrated *in vacuo* again to remove residual triphenylphosphine oxide to obtain a yellow oil. This was dissolved in hexane, passed through a silica plug and concentrated *in vacuo* to obtain the pure product, **S2**, as a colourless oil (81.6 g, 330 mmol, 90%). ^{1}H NMR data is consistent with the literature.[13]

^{1}H NMR (400 MHz, $CDCl_3$) δ 3.47 (d, J = 4.8 Hz, 2H), 1.65-1.45 (m, 1H), 1.45 – 1.22 (m, 16H), 0.95 – 0.89 (m, 6H).

1,2-Bis(2-butyloctyloxy)benzene [S4]

Adapted from a literature procedure.[14] However, we note that we could obtain only negligible yield using THF as the solvent as given in the original procedure.

Catechol, **S3**, (2.5 g, 23 mmol) and a spatula tip of Bu_4NBr were dissolved in 500 mL of dry DMF. NaH (2.0 g, 0.5 mmol, 2.2 eq.) was added as a single solid portion, producing a dark blue solution. The reaction mixture was heated to 80 °C for 30 minutes and observed to form a blue-grey suspension. **S2** (21 g, 84mmol, 3.7 eq.) was then added dropwise over a period of 2 h, and then the mixture was stirred at 80 °C for an additional 40 h, during which it transformed to a brown solution. The reaction mixture

was allowed to cool to room temperature and diluted with hexane (500 mL) and 0.1 M HCl (500 mL). The layers were separated and the aqueous layer extracted with hexane (3 x 100 mL). The combined organics were washed with brine (2 x 200 mL), sat. aq. $NaHCO_3$ (200 mL) and brine again (200 mL), and then dried ($MgSO_4$) and concentrated *in vacuo*. The crude product was dissolved in DCM, passed through a silica plug and concentrated *in vacuo.* Remaining impurities, including excess **S2**, were removed by Kugelrohr distillation to leave the pure product **S4** as a colourless oil (7.33 g, 16.4 mmol, 71%).

^{1}H NMR (500 MHz, $CDCl_3$) δ 6.93 (s, 4H), 3.90 (d, J=5.7 Hz, 4H), 1.89-1.84 (m, 2H), 1.60-1.53 (m, 4H), 1.48-1.32 (m,28H), 0.97-0.93 (m, 12H).

^{13}C NMR (126 MHz, $CDCl_3$) δ 149.7, 120.9, 113.9, 71.9, 38.2, 32.0, 31.4, 31.1, 29.8, 29.2, 26.9, 23.2, 22.8, 14.2, 14.1.

HRMS(m/z) Found [M+H]+ = 447.4199, $C_{30}H_{55}O_2$ requires 447.4202, Δ = -0.7 ppm

1,2-dibromo-4,5-bis((2-butyloctyl)oxy)benzene [2]

Adapted from a literature procedure for the ethylhexyl analogue.[15]

S4 (4.5 g, 10 mmol) was dissolved in a mixed solvent system of chloroform (60 mL) and methanol (60 mL) and cooled to 0 °C. A solution of bromine (1.1 mL, 3.4 g, 22 mmol, 2.2 eq.) in glacial acetic acid (40 mL) was added dropwise and the mixture was stirred for 2 h while maintaining the temperature at 0 °C. The reaction mixture was basified by the careful addition of aq. Na_2CO_3 (37 g in 200 mL H_2O) and the layers were separated. The organic layer was washed with aq. Na_2SO_4, dried ($MgSO_4$) and concentrated *in vacuo*. The crude product was purified by flash column chromatography using neat n-hexane as the eluent, to obtain **2** as a colourless oil (5.7 g, 9.4 mmol, 94%).

^{1}H NMR (500 MHz, $CDCl_3$) δ 7.08 (s, 2H), 3.84 (d, J=5.7 Hz, 4H), 1.85-1.80 (m, 2H), 1.54-1.28 (m,32H), 0.95-0.91 (m, 12H).

^{13}C NMR (126 MHz, $CDCl_3$) δ 149.4, 117.7, 114.4, 72.1, 38.0, 31.09 31.3, 31.0, 29.8, 29.1, 26.9, 23.1, 22.7, 14.1, 14.1.

HRMS(m/z) Found [M+H]+ = 602.2333, $C_{30}H_{53}O_2Br_2$ requires 602.2334, Δ = -0.2 ppm

ii) Synthesis of an Asymmetric Borylated DPH Intermediate [1]

Scheme S2

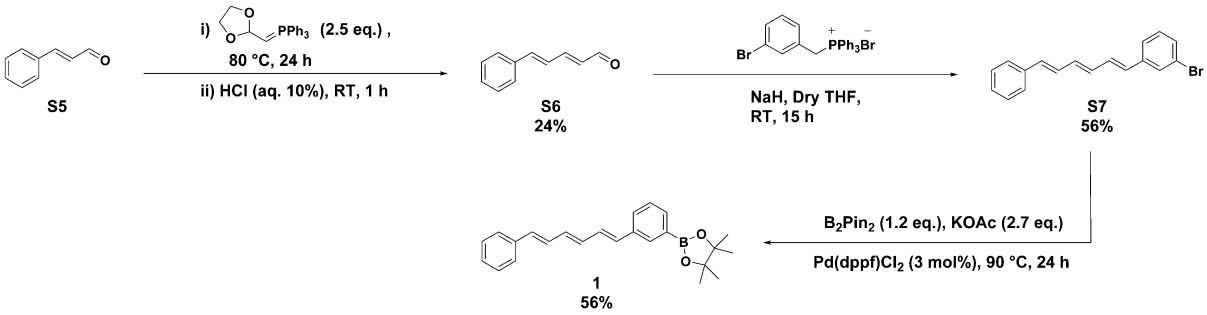

(2E,4E)-5-phenylpenta-2,4-dienal [S6]

To an oven-dried flask under an argon atmosphere and equipped with a dropping funnel and reflux condenser was added (1,3-dioxolan-2-ylmethyl)triphenylphosphonium bromide (28g, 65 mmol, 2.6 equiv.), and anh. THF (~500 mL) via cannula. To this was added lithium methoxide solution in methanol (2.2 M, 28.4 mL, 62 mmol, 2.5 equiv.). The suspension was heated to reflux (80 °C) for 30 mins. To a separate oven-dried flask under argon was added **S5** (3.3 g, 25 mmol, 1.0 equiv.) and anh. THF (~100 mL). This solution was transferred to the dropping funnel and added to reaction mixture over 30-60 mins. The mixture was heated to reflux and allowed to stir for 24 h. The reaction was cooled to RT, at which point 10% aq. HCl solution (100 mL) was added. Stirring was continued for 1 hr to hydrolyse intermediate acetals to the all-trans aldehydes. Colour change observed was from cloudy cream to clear and pale yellow. The organic layer was then separated, and the aqueous layer extracted with EtOAc. Combined organic layers were subsequently washed with water, sat. aq. sodium bicarbonate solution and brine, before being dried ($MgSO_4$) and concentrated *in vacuo*. The crude material was then stirred in *n*-hexane (~ 500 mL) overnight and filtered through celite to remove insoluble phosphine oxide by-product. The filtrate was concentrated *in vacuo* and purified by flash column chromatography (eluent: DCM/ *n*-hexane gradient from 0:100 → 15:85 v/v), to give the title product, **S6**, as a yellow oil, (0.95 g, 6.0 mmol, 24%), following removal of the solvent. ^{1}H and ^{13}C NMR data are consistent with the literature.[16]

^{1}H NMR (400 MHz, $CDCl_3$) δ 9.65 (d, J = 7.9 Hz, 1H), 7.55 – 7.52 (m, 2H), 7.44-7.35 (m, 3H), 7.30 (ddd, J = 15.2, 7.4, 2.9 Hz, 1H), 7.05-7.03 (m, 2H), 6.30 (dd, J = 15.2, 7.9 Hz, 1H).

^{13}C NMR (101 MHz, $CDCl_3$) δ 193.6, 152.0, 142.4, 135.6, 131.7, 129.7, 129.0, 127.5, 126.2.

1-bromo-3-((1E,3E,5E)-6-phenylhexa-1,3,5-trien-1-yl)benzene [S7]

S7 was synthesized by a Wittig reaction of pentadienal **S6** and phosphonium salt, 3-bromobenzyl triphenylphosphonium bromide (prepared as previously reported)[1]. Sodium hydride (60% dispersion in mineral oil, 552 mg, 13.8 mmol, 2.3 eq.) was dissolved in dry THF (250 mL) and cooled to 0 °C using an ice bath, under argon. Under a positive flow of argon, the phosphonium salt (3.8 g, 7.5 mmol, 1.25 eq.) was added as a single solid portion. The ice bath was removed, and the suspension was stirred at room temperature for 15 minutes. Colour change from the immediately formed yellow suspension to orange was observed. A solution of **S6** (0.95 g, 6.0 mmol, 1.0 eq.) in dry THF (40 mL) was prepared and added dropwise and the mixture stirred overnight, in the dark. The mixture was poured over ice/brine, diluted with EtOAc and the layers separated. The organic layer was washed with 1 M HCl (100 mL) and brine (100 mL), dried ($MgSO_4$) and the solvent removed *in vacuo.* The solid material was sonicated in methanol, filtered, washed with more methanol and dried under suction. **S8** was obtained as a pale-yellow powder (1.05 g, 3.36 mmol, 56%).

^{1}H NMR (500 MHz, $CDCl_3$) δ 7.59 (t, *J* = 1.8 Hz, 1H), 7.45(d, *J* = 7.3 Hz, 2H), 7.37-7.34 (m, 4H), 7.25 (tt, *J* = 7.5, 1.3 Hz, 1H), 7.21 (t, *J* = 7.5 Hz, 1H), 6.91 (ddd, *J* = 15.5, 10.1, 8.0 Hz, 2H), 6.67 – 6.50 (m, 4H).

^{13}C NMR (126 MHz, $CDCl_3$): δ 139.6, 137.2, 134.7, 133.4, 133.0, 130.9, 130.5, 130.3, 130.1, 129.1, 128.9, 128.7, 127.7, 126.5, 125.0, 122.9.

HRMS(m/z) Found [M+H]+ = 311.0434, $C_{18}H_{16}Br$ requires 311.0435, Δ = -0.3 ppm

4,4,5,5-tetramethyl-2-(3-((1E,3E,5E)-6-phenylhexa-1,3,5-trien-1-yl)phenyl)-1,3,2-dioxaborolane [1]

1 was prepared by a Miyaura borylation from the bromide **S7**. **S7** (1.0 g, 3.35 mmol, 1.0 eq.), bis(pinacolato)diboron (1.02 g, 4.0 mmol, 1.2 eq.), Pd(dppf)Cl_2 (74 mg, 0.1 mmol, 0.03 eq.), potassium acetate (886 mg, 9.0 mmol, 2.7 eq.) and stir bar were added to a Schlenk flask, which was evacuated and backfilled with argon 5 times. Dry dioxane (50 mL) was added, the reaction mixture was lowered into a preheated oil bath and stirred at 90 °C in the dark for 24 h. The reaction mixture was allowed to cool to room temperature and then the solvent removed *in vacuo*. The crude material was dissolved in DCM, dry loaded onto silica and purified by flash column chromatography (eluent: DCM/ *n*-hexane gradient from 0:100 → 30:70 v/v). After removal of the solvent, the material was sonicated in MeOH, filtered and dried under suction to obtain the product, **1,** as an off-white powder (670 mg, 1.9 mmol, 56%).

^{1}H NMR (500 MHz, $CDCl_3$) δ 7.90 (s, 1H), 7.70 (dt, *J* = 7.3, 1.2 Hz, 1H), 7.54 (dt, *J* = 7.8, 1.9 Hz, 1H), 7.45(d, *J* = 7.1 Hz, 2H), 7.38-7.34 (m, 3H), 7.25 (tt, *J* = 7.4, 1.2 Hz, 1H), 7.21 (t, *J* = 7.5 Hz, 1H), 7.00-6.90 (m, 2H), 6.64 (d, *J* = 15.6 Hz, 1H), 6.63 (d, *J* = 15.6 Hz, 1H), 6.59 – 6.52 (m, 2H), 1.39 (s, 12H).

^{13}C NMR (126 MHz, $CDCl_3$): δ 137.4, 136.7, 133.9, 133.8, 133.5, 132.8, 132.7, 132.6, 129.2, 129.2, 128.7, 128.1, 127.5, 126.4, 83.9, 24.9.

HRMS(m/z) Found [M+H]+ = 358.2117, $C_{24}H_{28}BO_2$ requires 358.2104, Δ = 3.6 ppm

iii) Synthesis of a Symmetric Diborylated DPH Intermediate [3]

Scheme S3

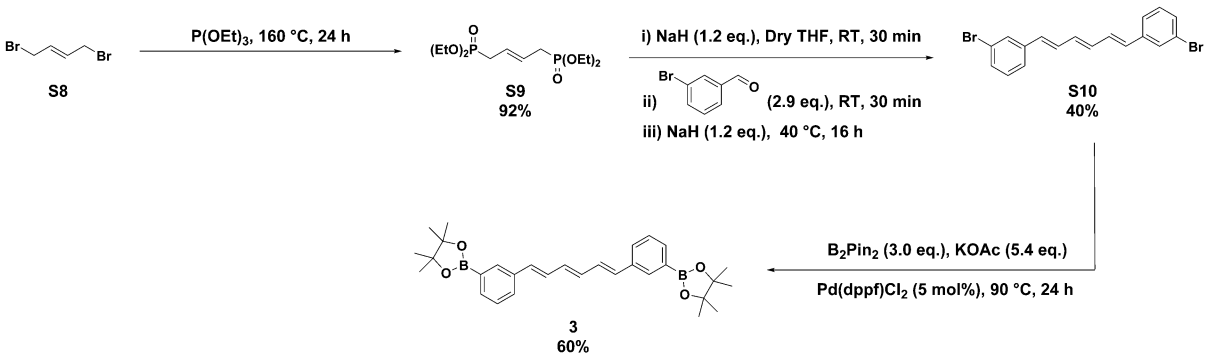

tetraethyl but-2-ene-1,4-diyl(E)-bis(phosphonate) [S9]

To an oven-dried flask set up for reflux and under an argon atmosphere was added 1,4-dibromo-2-butene, **S8**, (10 g, 47 mmol, 1.0 equiv.) and triethyl phosphite (19 mL, 110 mmol, 2.4 equiv.). The mixture was heated to 160 ^{o}C and stirred for 24 h. The resulting mixture was cooled to RT, and volatile impurities removed by Kugelrohr distillation to leave **S9** as a brown oil, (14.8 g, 45 mmol, 97%).^{1}H and ^{13}C NMR data are consistent with the literature.[17]

^{1}H NMR (500 MHz, $CDCl_3$) δ 5.64-5.61 (m, 2H), 4.15-4.08 (m, 8H), 2.67-2.57 (m, 4H), 1.33 (t, *J* = 7.1 Hz, 12H).

^{13}C NMR (126 MHz, $CDCl_3$): δ 124.3 (t, $^{2}J_{P\text{-}C}$ = 4.0 Hz), 61.9 (t, $^{2}J_{P\text{-}C}$ = 3.2 Hz), 30.6 (dd, $^{1}J_{P\text{-}C}$ = 142 Hz, $^{4}J_{P\text{-}C}$ = 4.3 Hz,), 16.5 (t, $^{3}J_{P\text{-}C}$ = 3.0 Hz).

(1E,3E,5E)-1,6-bis(3-bromophenyl)hexa-1,3,5-triene [S10]

To an oven-dried flask under argon was added **S9** (8.12 g, 24.7 mmol, 1.0 equiv.) and anh. THF (~250 mL). Sodium hydride (60% dispersion in mineral oil, 1.19 g, 29.7 mmol, 1.2 eq.) was then added as a single portion and the resulting mixture was allowed to stir at RT for 30 mins. To this, 3-bromobenzaldehyde (8.4 mL, 13.3 g, 72 mmol, 2.9 equiv.) was added dropwise over 5 mins and then left to stir for 30 mins at RT. A second dose of sodium hydride (60% dispersion in mineral oil, 1.19 g, 29.7 mmol, 1.2 eq.) was added as a single portion, the reaction mixture warmed to 40 °C and stirred for 16 h in the dark. The reaction mixture was cooled to 0 °C and filtered. The precipitate was washed with water (~50 mL) followed by methanol (~20 mL). The precipitate was then dissolved in boiling THF and filtered, while hot, to remove insoluble impurities. The filtrate was concentrated *in vacuo* and then recrystallized from THF (boiling → -17 °C). The product, **S10**, crystallized as bright yellow needles, which were filtered, washed with MeOH and dried under suction to yield **S10** (3.84 g, 9.85 mmol, 40%).

^{1}H NMR (500 MHz, $CDCl_3$) δ 7.59 (t, *J* = 1.9 Hz, 2H), 7.37 (d, *J* = 7.9 Hz, 2H), 7.34 (d, *J* = 7.8 Hz, 2H), 7.21 (t, *J* = 7.8 Hz, 2H), 6.89 (ddd, *J* = 15.5, 7.0, 3.3 Hz, 2H), 6.58 – 6.51 (m, 4H).

^{13}C NMR (126 MHz, $CDCl_3$): δ 139.5, 134.0, 131.6, 130.4, 130.3, 130.2, 129.1, 125.1, 122.9.

HRMS(m/z) Found [M+H]+ = 388.9537, $C_{18}H_{15}Br_2$ requires 388.9541, Δ = -1.0 ppm

(1E,3E,5E)-1,6-bis(3-(4,4,5,5-tetramethyl-1,3,2-dioxaborolan-2-yl)phenyl)hexa-1,3,5-triene [3]

3 was prepared by a Miyaura borylation from the dibromide **S10**. **S10** (1.22 g, 3.13 mmol, 1.0 eq.), bis(pinacolato)diboron (2.4 g, 9.4 mmol, 3.0 eq.), $Pd(dppf)Cl_2$ (120 mg, 0.16 mmol, 0.05 eq.), potassium acetate (1.95 g, 19.9 mmol, 6.3 eq.) and stir bar were added to a Schlenk flask, which was evacuated and backfilled with argon 5 times. Dry dioxane (~75 mL) was added, the reaction mixture was lowered into a preheated oil bath and stirred at 90 °C in the dark for 24 h. The reaction mixture was allowed to cool to room temperature and then the solvent removed *in vacuo*. The crude material was dissolved in DCM, dry loaded onto silica and purified by flash column chromatography (eluent: DCM/ *n*-hexane 80:20 v/v). After removal of the solvent, the material was sonicated in MeOH, filtered and dried under suction to obtain the product, **3,** as a cream-coloured powder (1.2 g, 25 mmol, 80%).

^{1}H NMR (500 MHz, $CDCl_3$) δ 7.90 (s, 2H), 7.70 (d, *J* = 7.3 Hz 2H), 7.54 (d, *J* = 7.8 Hz, 2H), 7.36(t, *J* = 7.5 Hz, 2H), 6.98 (ddd, *J* = 15.6, 7.1, 3.2 Hz, 2H), 6.64 (d, *J* = 15.5 Hz, 2H), 6.58 – 6.52 (m, 2H), 1.39 (s, 24H).

^{13}C NMR (126 MHz, $CDCl_3$): δ 136.8, 133.9, 133.6, 132.8, 132.6, 129.3, 129.2, 128.1, 83.9, 24.9.

HRMS(m/z) Found [M]+ = 484.2975, $C_{30}H_{38}B_2O_4$ requires 484.2956, Δ = 3.9 ppm

iv) Oligomer Syntheses

Scheme S4. Reproduced from Scheme 1 for ease of referral.

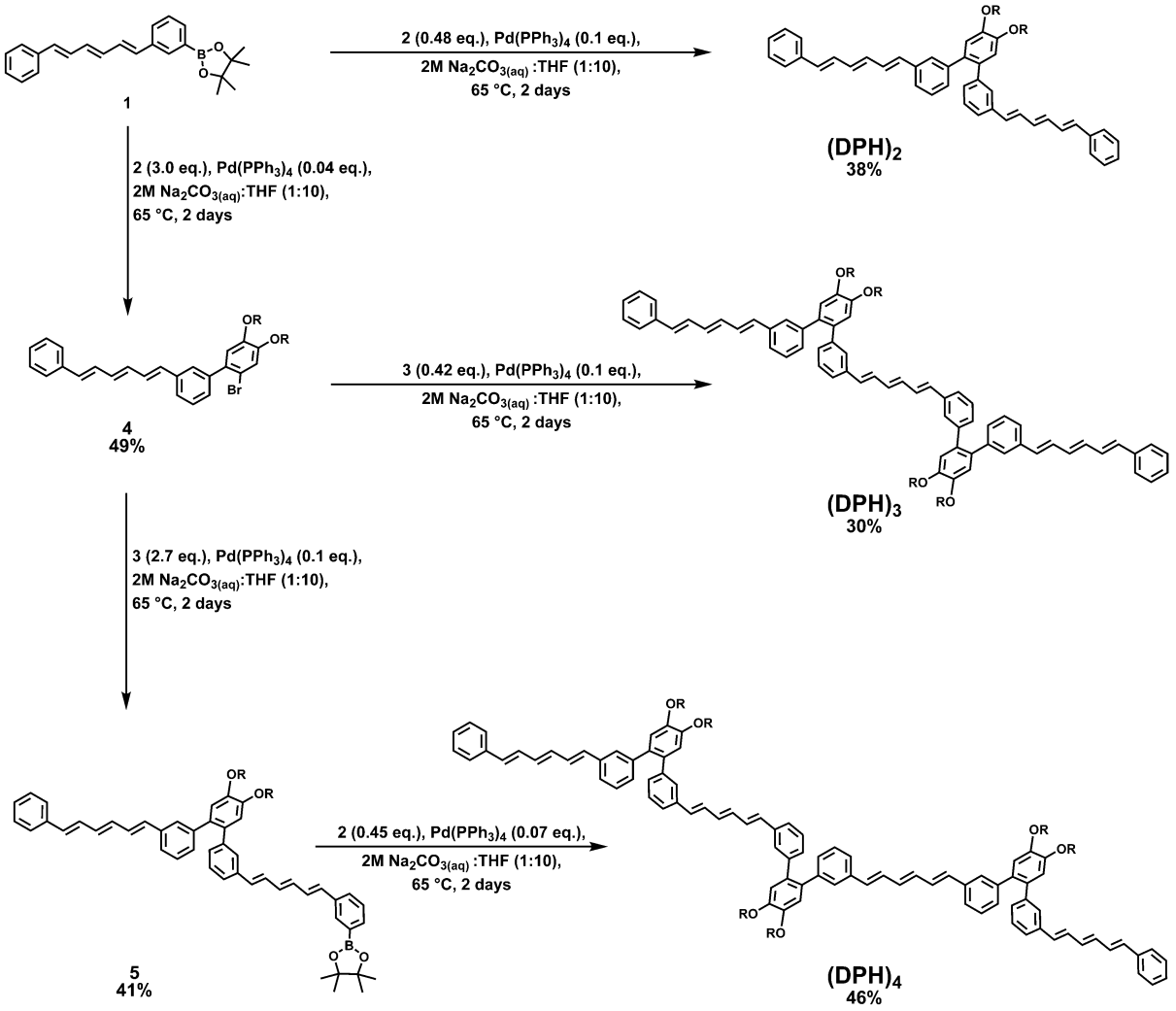

4',5'-bis((2-butyloctyl)oxy)-3,3''-bis((1E,3E,5E)-6-phenylhexa-1,3,5-trien-1-yl)-1,1':2',1''-terphenyl [$(DPH)_2$]

A 20 mL microwave vial was charged with a stir bar, **1** (122 mg, 0.34 mmol, 2.1 eq.), and $Pd(PPh_3)_4$ (17 mg, 0.016 mmol, 0.1 eq.) and flushed under argon. A solution of **2** (95 mg, 0.16 mmol, 1.0 eq.) in THF (10 mL) and an aqueous solution of Na_2CO_3 (2M, 1 mL) were separately degassed and then added to the solid reagents. The reaction mixture was lowered into a preheated oil bath and heated at 65 °C in the dark for 2 days. The reaction mixture was carefully acidified with 1 M HCl (~ 4 mL) with stirring and then diluted with DCM (~100 mL) and brine (~75 mL). The organic layer was separated and washed with brine (~ 30 mL), dried ($MgSO_4$) and the solvent remove *in vacuo*. The crude material was then purified by flash column chromatography (eluent: DCM/ *n*-hexane gradient from 0:100 → 40:60 v/v). Following removal of the solvent the columned material was sonicated in methanol, filtered, and then

recrystallized from EtOH/ $CHCl_3$ to obtain the product, **(DPH)$_2$**, as a yellow powder (54.7 mg, 0.060 mmol, 38%).

^{1}H NMR (500 MHz, $CDCl_3$) δ 7.44 (d, *J* = 7.5 Hz, 4H), 7.32-7.29 (m, 6H), 7.26-7.21 (m, 4H), 7.17 (t, *J* = 7.7 Hz, 2H), 7.00-6.99 (m, 4H), 6.91 (dd, *J* = 15.6, 9.8 Hz, 2H), 6.71 (dd, *J* = 15.4, 9.9 Hz, 2H), 6.63 – 6.47 (m, 8H), 3.97 (d, J=5.7 Hz, 4H), 1.92-1.85 (m, 2H), 1.59-1.29 (m,32H), 0.96-0.90 (m, 12H).

^{13}C NMR (126 MHz, $CDCl_3$): δ 148.9, 141.9, 137.4, 137.0, 133.7, 133.6, 132.9, 132.8, 132.7, 129.3, 129.3, 129.1, 128.6, 128.2, 127.5, 126.4, 124.4, 115.5, 72.1, 38.2, 32.0, 31.4, 31.1, 29.8, 29.1, 26.9, 23.1, 22.8, 14.2, 14.2.

HRMS(m/z) Found [M+H]+ = 907.6389, $C_{66}H_{83}O_2$ requires 907.6393, Δ = -0.4 ppm

2-bromo-4,5-bis((2-butyloctyl)oxy)-3'-((1E,3E,5E)-6-phenylhexa-1,3,5-trien-1-yl)-1,1'-biphenyl [4]

Compound **4** was prepared by an analogous Suzuki coupling procedure to **(DPH)$_2$**, except inverting the excess reagent and on a larger scale. **1** (270 mg, 0.75 mmol, 1.0 eq.), $Pd(PPh_3)_4$ (50 mg, 0.04 mmol, 0.06 eq.), **2** (1.36 g, 2.25 mmol, 3.0 eq.) in THF (30 mL) and aq. Na_2CO_3 (2M, 3 mL) were utilized. The product, **4,** was collected at a solvent composition of 20:80 DCM/ *n*-hexane (v/v) during flash column chromatography. The resultant green oil was sonicated in MeOH and observed to coalesce into a yellow-green globule. The MeOH was decanted off, and the material dried under vacuum. **4**, containing a small amount of isomer impurity which was carried over into the next steps, was obtained as a green oil (277 mg, 0.366 mmol, 49%).

^{1}H NMR (500 MHz, $CDCl_3$) δ 7.50 (s, 1H), 7.47-7.44 (m, 3H), 7.41 (t, *J* = 7.6 Hz, 1H), 7.36 (t, *J* = 7.7 Hz, 2H), 7.31 (dt, *J* = 7.4, 1.5 Hz, 1H), 7.26 (tt, *J* = 7.4, 1.3 Hz, 1H), 7.17 (s, 1H), 7.00-6.91 (m, 2H), 6.71-6.63 (m, 2H), 6.61 – 6.54 (m, 2H), 3.93 (d, J=5.7 Hz, 2H), 3.89 (d, J=5.7 Hz, 2H), 1.91-1.83 (m, 2H), 1.60-1.31 (m,32H), 0.99-0.92 (m, 12H).

^{13}C NMR (126 MHz, $CDCl_3$): δ 149.5, 148.8, 141.7, 137.4, 137.2, 134.4, 133.8, 133.6, 132.8, 132.5, 129.5, 129.1, 128.9, 128.7, 128.3, 127.6, 127.6, 126.4, 125.3, 117.6, 115.9, 112.3, 72.1, 72.2, 38.2, 38.1, 32.0, 31.9, 31.4, 31.4, 31.1, 31.1, 29.8, 29.8, 29.1, 29.1, 26.9, 23.1, 23.1, 22.8, 22.8, 14.2, 14.2, 14.2, 14.2.

HRMS(m/z) Found [M]+ = 754.4307, $C_{48}H_{67}O_2Br$ requires 754.4324, Δ = -2.3 ppm

(1E,3E,5E)-1,6-bis(4',5'-bis((2-butyloctyl)oxy)-3''-((1E,3E,5E)-6-phenylhexa-1,3,5-trien-1-yl)-[1,1':2',1''-terphenyl]-3-yl)hexa-1,3,5-triene [$(DPH)_3$]

$(DPH)_3$ was prepared by a similar Suzuki coupling procedure to **$(DPH)_2$**. A flask was charged with **3** (23 mg, 0.048 mmol, 1.0 eq.), **4** (86 mg, 0.110 mmol, 2.4 eq.) and $Pd(PPh_3)_4$ (6 mg, 0.005 mmol, 0.1 eq.). Separately degassed THF (5 mL) and aq. Na_2CO_3 (2M, 0.5 mL) were added. Following reaction for 2 days at 65 °C in the dark and an analogous aqueous work-up to that above, the crude material was purified by flash column chromatography (eluent: DCM/ *n*-hexane gradient from 0:100 → 25:75 v/v). Following removal of the solvent the material was sonicated in methanol, filtered and washed with a small volume of hexanes. **$(DPH)_3$** was obtained as a beige powder (23 mg, 0.015 mmol, 30%).

^{1}H NMR (500 MHz, $CDCl_3$) δ 7.40 (d, *J* = 7.4 Hz, 4H), 7.34(s, 2H), 7.30-7.7.19 (m, 12H), 7.16 (t, *J* = 7.6 Hz, 2H), 7.12 (t, *J* = 7.7 Hz, 2H), 7.02-6.98 (m, 8H), 6.90 (dd, *J* = 15.6, 9.8 Hz, 2H), 6.77 – 6.61 (m, 4H), 6.61 – 6.46 (m, 12H), 3.99 (d, J=5.7 Hz, 4H), 3.97 (d, J=5.7 Hz, 4H), 1.93-1.88 (m, 4H), 1.61-1.30 (m,64H), 0.98-0.92 (m, 24H).

^{13}C NMR (126 MHz, $CDCl_3$): δ 148.9, 141.9, 141.9, 137.3, 137.0, 133.8, 133.6, 132.9, 132.8, 132.8, 132.8, 132.6, 129.3, 129.2, 129.1, 128.6, 128.2, 128.1, 128.0, 127.5, 126.4, 124.6, 124.4, 115.5, 72.1, 38.3, 32.0, 31.5, 31.1, 29.8, 29.2, 27.0, 23.2, 22.8, 14.2.

HRMS(m/z) Found [M+H]+ = 1582.1403, $C_{114}H_{149}O_4$ requires 1582.1456, Δ = -3.3 ppm

2-(3-((1E,3E,5E)-6-(4',5'-bis((2-butyloctyl)oxy)-3''-((1E,3E,5E)-6-phenylhexa-1,3,5-trien-1-yl)-[1,1':2',1''-terphenyl]-3-yl)hexa-1,3,5-trien-1-yl)phenyl)-4,4,5,5-tetramethyl-1,3,2-dioxaborolane [5]

Compound **5** was prepared by a similar Suzuki coupling procedure. **3** (500 mg, 1.0 mmol, 2.7 eq.), $Pd(PPh_3)_4$ (43 mg, 0.037 mmol, 0.1 eq.), a solution of **4** (277 mg, 0.366 mmol, 1.0 eq.) in THF (15 mL) and aq. Na_2CO_3 (2M, 1.5 mL) were utilized. After the reaction period of 2 day at 65 °C in the dark, the reaction mixture was NOT acidified. The layers were separated directly, and the aqueous layer extracted with Et_2O. The combined organics were dried ($MgSO_4$) and the solvent remove *in vacuo*. The crude material was then purified by flash column chromatography (eluent: DCM/ *n*-hexane gradient from 0:100 → 50:50 v/v, holding at 40:60 to remove **$(DPH)_2$** produced by deborylation of the target compound). The product, **5,** was sonicated in MeOH, filtered, and dried under vacuum. **5**, containing a small amount of isomer impurity which was carried over into the next step, was obtained as a cream-coloured powder (155 mg, 0.150 mmol, 41%).

^{1}H NMR (500 MHz, $CDCl_3$) δ 7.92 (s, 1H), 7.69 (d, *J* = 7.3 Hz, 1H), 7.50 (d, *J* = 7.7 Hz, 1H), 7.42 (d, *J* = 7.1 Hz, 2H), 7.34-7.15 (m, 8H), 7.18 (t, *J* = 7.7 Hz, 1H), 7.16 (t, *J* = 7.7 Hz, 1H), 7.04-6.96 (m, 5H), 6.90 (dd, *J* = 15.6, 9.9 Hz, 1H), 6.77 (dd, *J* = 15.4, 9.9 Hz, 1H), 6.69 (dd, *J* = 15.4, 9.9 Hz, 1H), 6.65 – 6.49 (m, 8H), 3.98 (d, J=5.7 Hz, 4H), 1.92-1.87 (m, 2H), 1.60-1.29 (m, 44H), 0.97-0.91 (m, 12H).

^{13}C NMR (126 MHz, $CDCl_3$): δ 148.9, 142.0, 141.9, 137.4, 137.1, 137.0, 136.7, 133.9, 133.8, 133.7, 133.6, 133.5, 132.8, 132.8, 132.7, 132.6, 132.6, 129.5, 129.3, 129.2, 129.1, 128.6, 128.2, 128.1, 128.1, 127.5, 126.4, 124.5, 124.3, 115.6, 83.9, 72.1, 38.2, 32.0, 31.5, 31.1, 29.8, 29.2, 26.9, 24.9, 23.2, 22.8, 14.2, 14.2.

HRMS(m/z) Found [M]+ = 1033.7189, $C_{72}H_{93}BO_4$ requires 1033.7245, Δ = -5.4 ppm

3'',3''''-((1E,1'E,3E,3'E,5E,5'E)-(4',5'-bis((2-butyloctyl)oxy)-[1,1':2',1''-terphenyl]-3,3''-diyl)bis(hexa-1,3,5-triene-6,1-diyl))bis(4',5'-bis((2-butyloctyl)oxy)-3-((1E,3E,5E)-6-phenylhexa-1,3,5-trien-1-yl)-1''',1'''':2'''',1''''-terphenyl) [(DPH)$_4$]

(DPH)$_4$ was prepared by a similar Suzuki coupling procedure and work up to **(DPH)$_2$**. **5** (130 mg, 0.126 mmol, 2.2 eq.), $Pd(PPh_3)_4$ (10 mg, 0.009 mmol, 0.15 eq.), **2** (34 mg, 0.057 mmol, 1.0 eq.) in THF (5 mL) and aq. Na_2CO_3 (2M, 0.5 mL) were utilized. Following the final recrystallization from EtOH/$CHCl_3$, **(DPH)$_4$** was obtained as a pale yellow powder (60 mg, 0.026 mmol, 46%).

^{1}H NMR (500 MHz, $CDCl_3$) δ 7.38(d, *J* = 7.2 Hz, 4H), 7.31(s, 2H), 7.28-7.24 (m, 8H), 7.21-7.17 (m, 8H), 7.14-7.06 (m, 6H), 6.99-6.94 (m, 12H), 6.73 – 6.65 (m, 4H), 6.59 – 6.45 (m, 16H), 3.99 (d, J=5.7 Hz, 4H), 3.96-3.94 (m, 12H), 1.90-1.84 (m, 6H), 1.58-1.28 (m, 96H), 0.95-0.89 (m, 36H).

^{13}C NMR (126 MHz, $CDCl_3$): δ 148.8, 148.8, 141.8, 141.8, 137.3, 137.0, 137.0, 137.0, 133.7, 133.7, 133.5, 132.8, 132.8, 132.8, 132.7, 132.6, 129.3, 129.2, 129.2, 129.2, 129.0, 128.6, 128.2, 128.1, 128.0, 127.9, 127.9, 127.5, 126.4, 124.7, 124.5, 124.4, 115.5, 72.1, 38.2, 31.9, 31.4, 31.1, 29.8, 29.1, 26.9, 23.1, 22.7, 14.1, 14.1.

HRMS(m/z) Found [M+H]+ = 2256.6501, $C_{162}H_{215}O_6$ requires 2256.6519, Δ = -0.8 ppm

7. NMR Spectra

2-butyloctylbromide [2]

^{1}H NMR, 400 MHz, $CDCl_3$

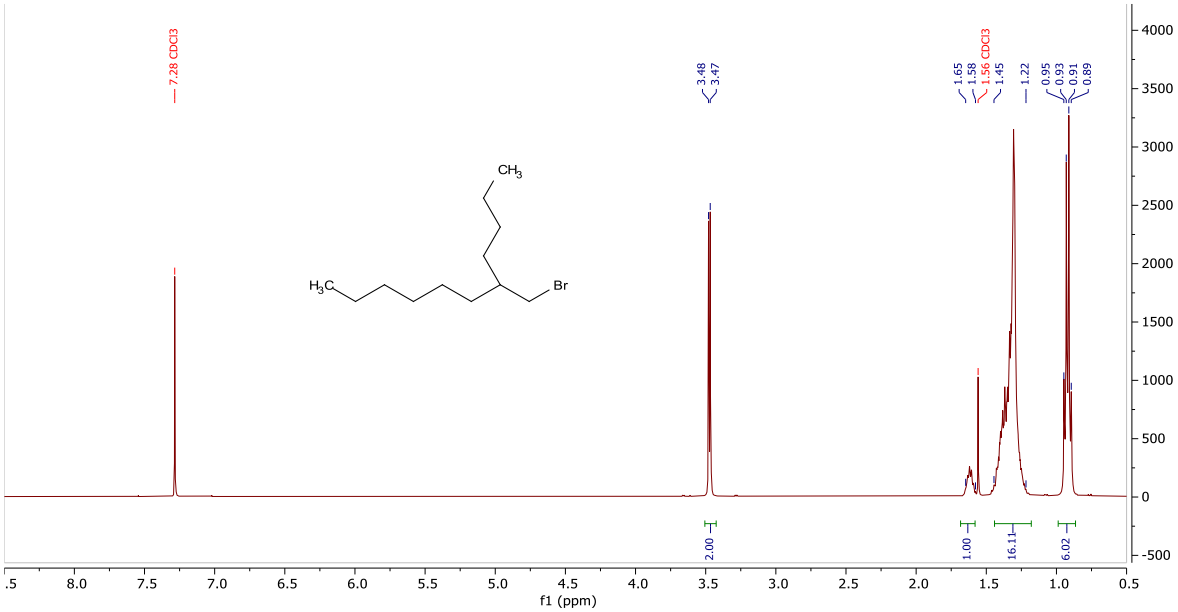

1,2-Bis(2-butyloctyloxy)benzene [4]

^{1}H NMR, 500 MHz, $CDCl_3$

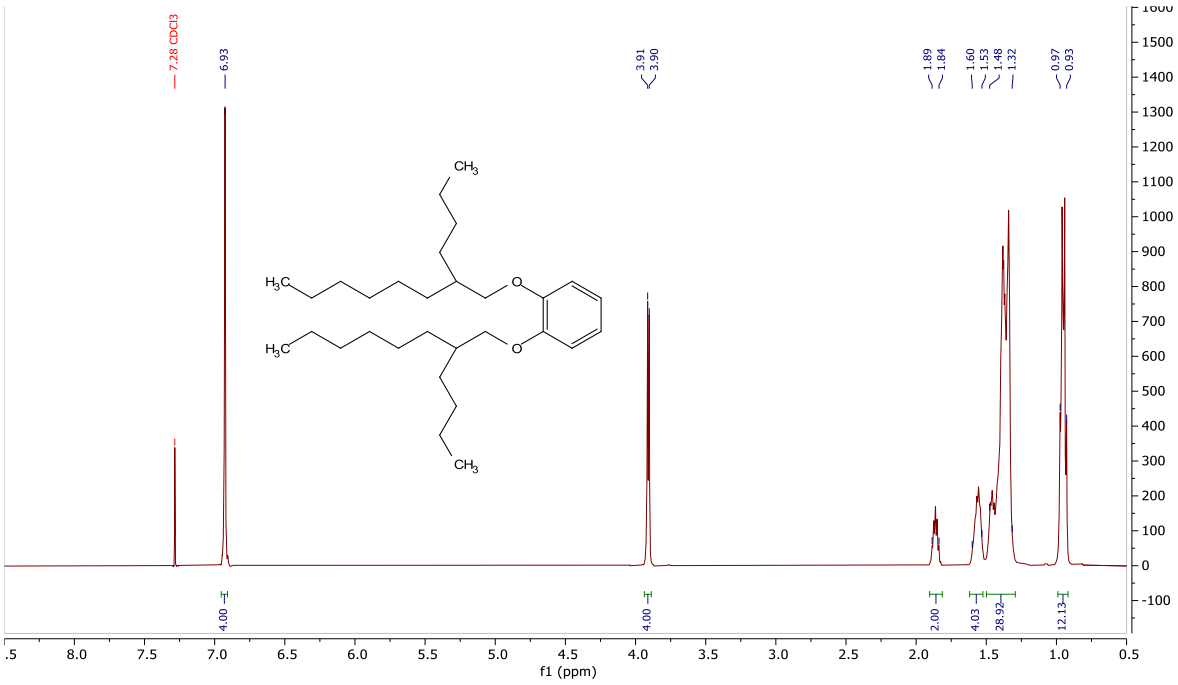

^{13}C NMR, 126 MHz, $CDCl_3$

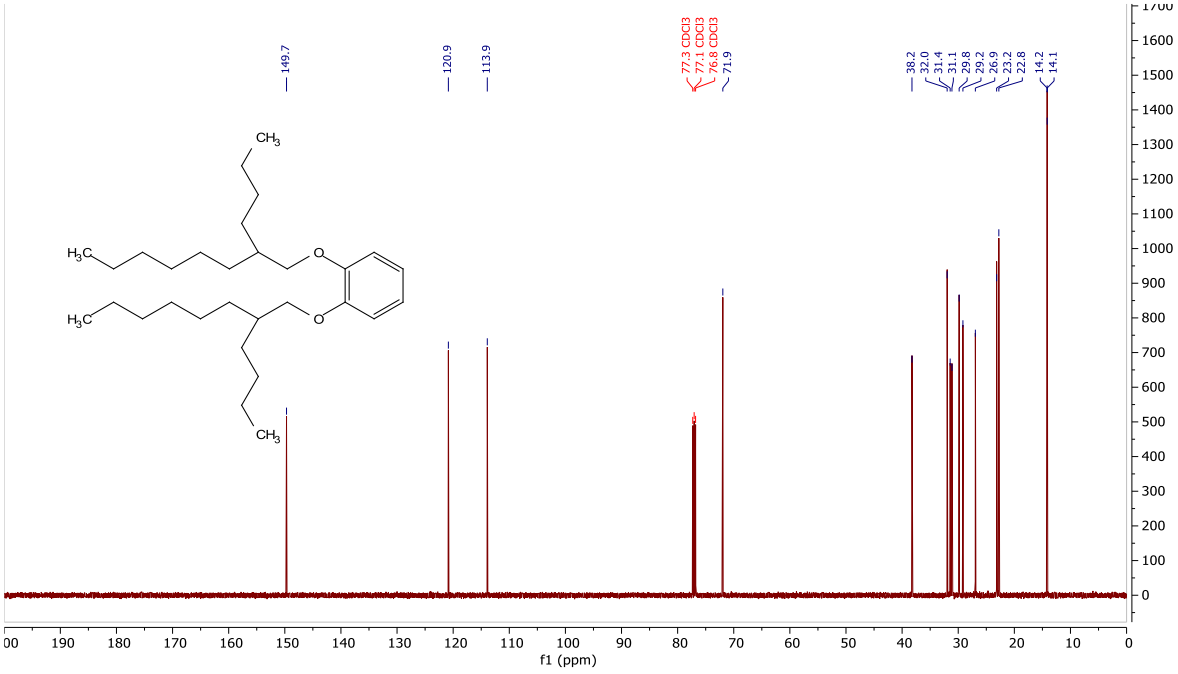

1,2-dibromo-4,5-bis((2-butyloctyl)oxy)benzene [5]

^{1}H NMR, 500 MHz, $CDCl_3$

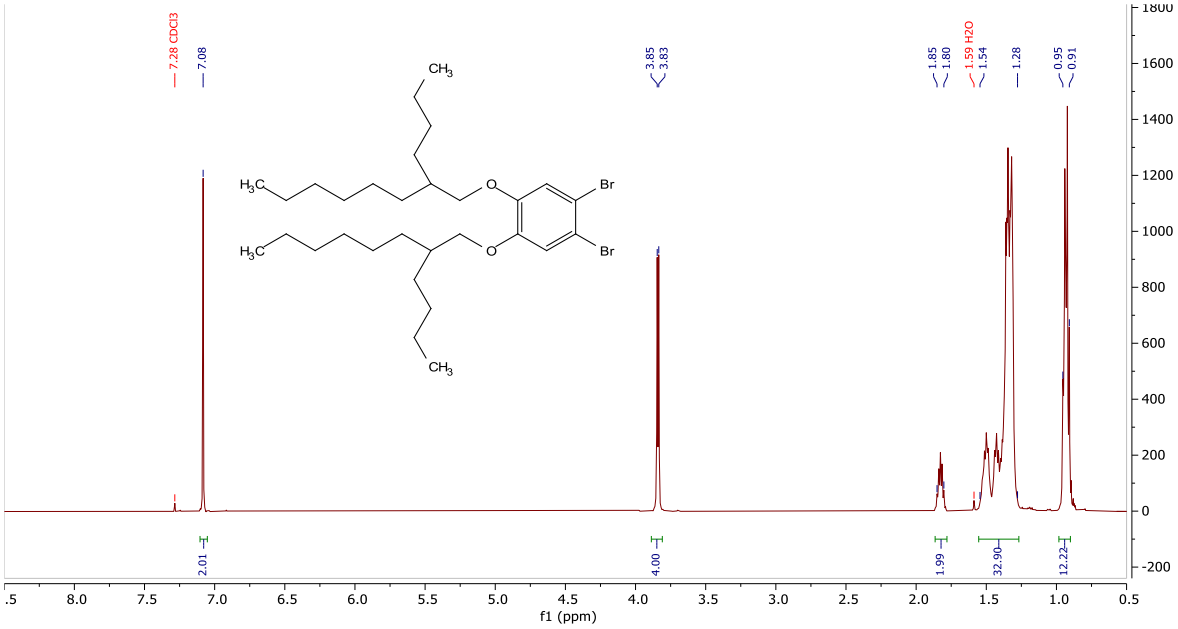

^{13}C NMR, 126 MHz, $CDCl_3$

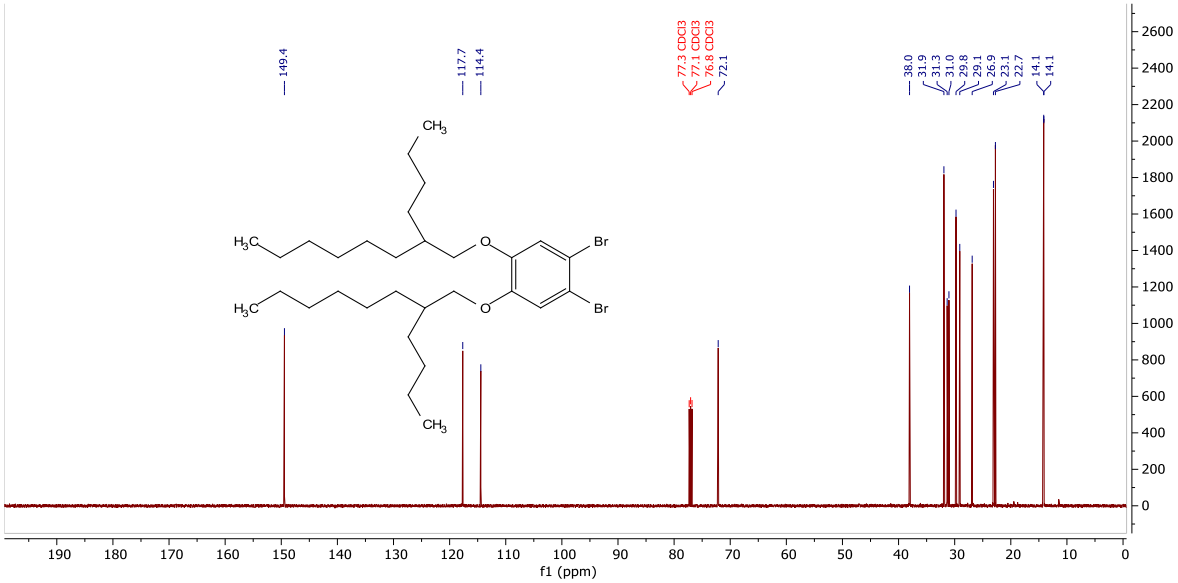

(2E,4E)-5-phenylpenta-2,4-dienal [7]

^{1}H NMR, 400 MHz, $CDCl_3$

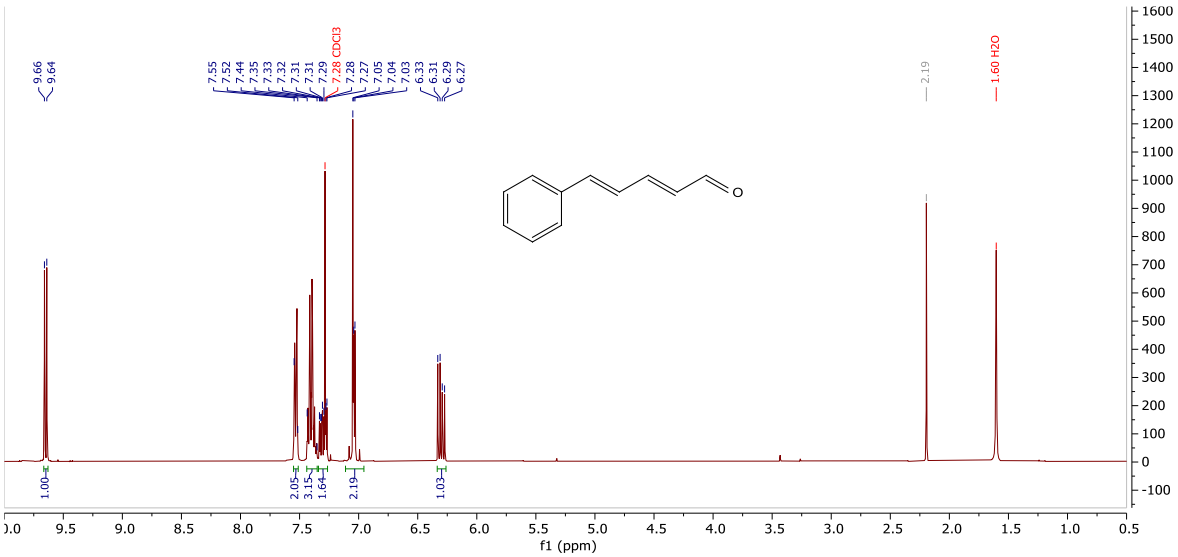

^{13}C NMR, 101 MHz, $CDCl_3$

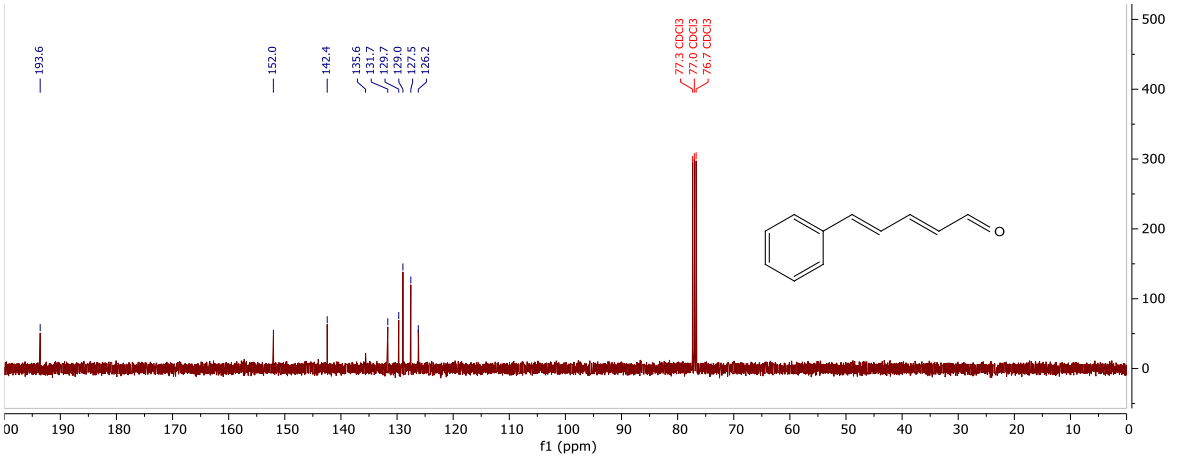

1-bromo-3-((1E,3E,5E)-6-phenylhexa-1,3,5-trien-1-yl)benzene [8]

^{1}H NMR, 500 MHz, $CDCl_3$

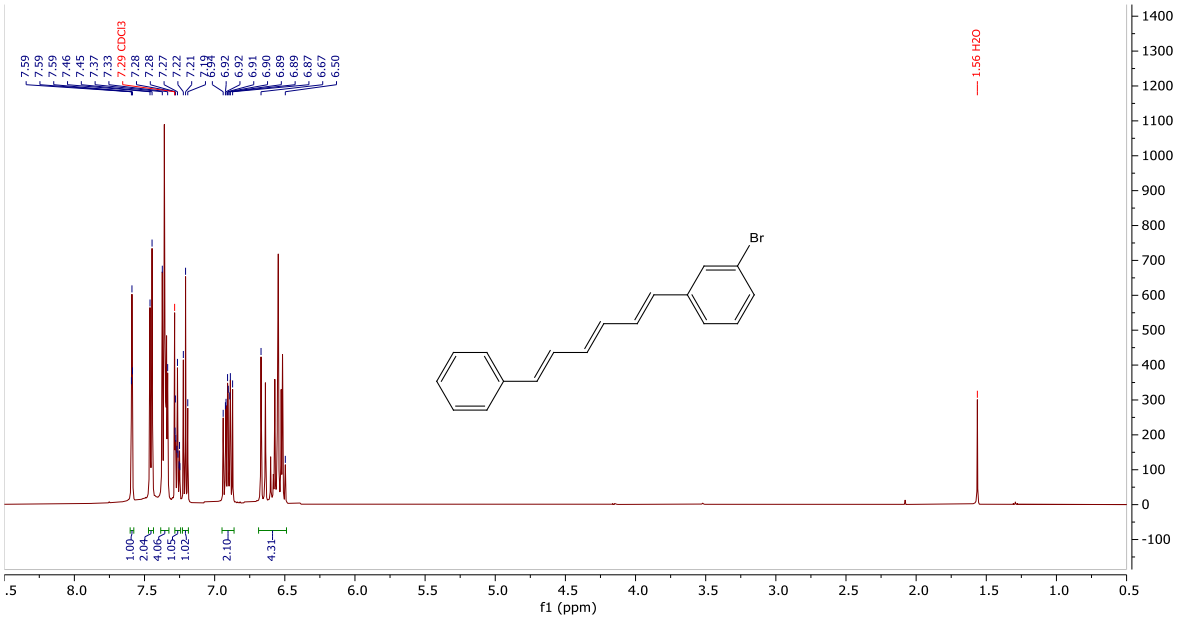

^{13}C NMR, 126 MHz, $CDCl_3$

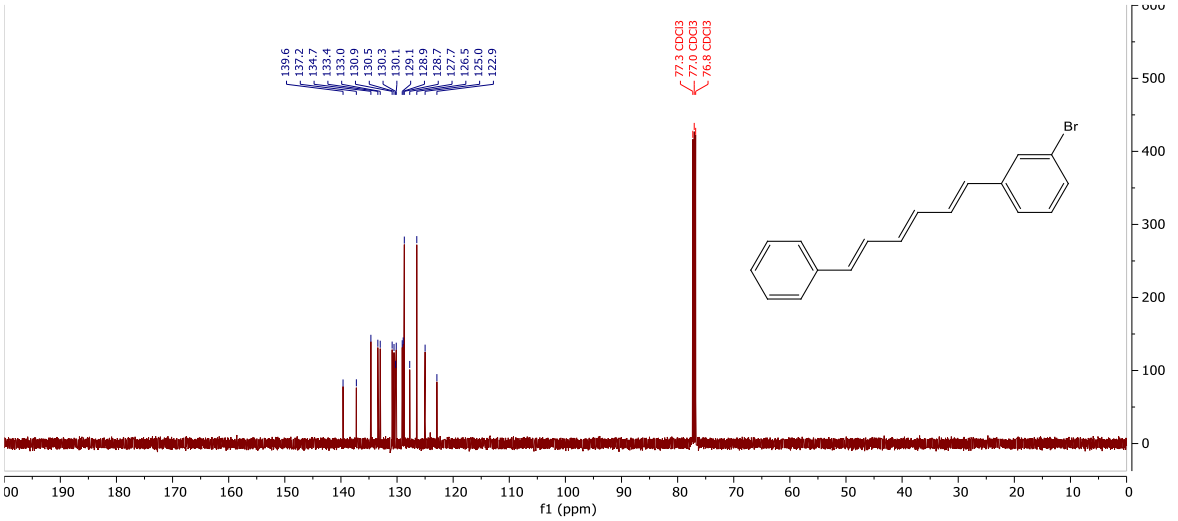

4,4,5,5-tetramethyl-2-(3-((1E,3E,5E)-6-phenylhexa-1,3,5-trien-1-yl)phenyl)-1,3,2-dioxaborolane [9]

^{1}H NMR, 500 MHz, $CDCl_3$

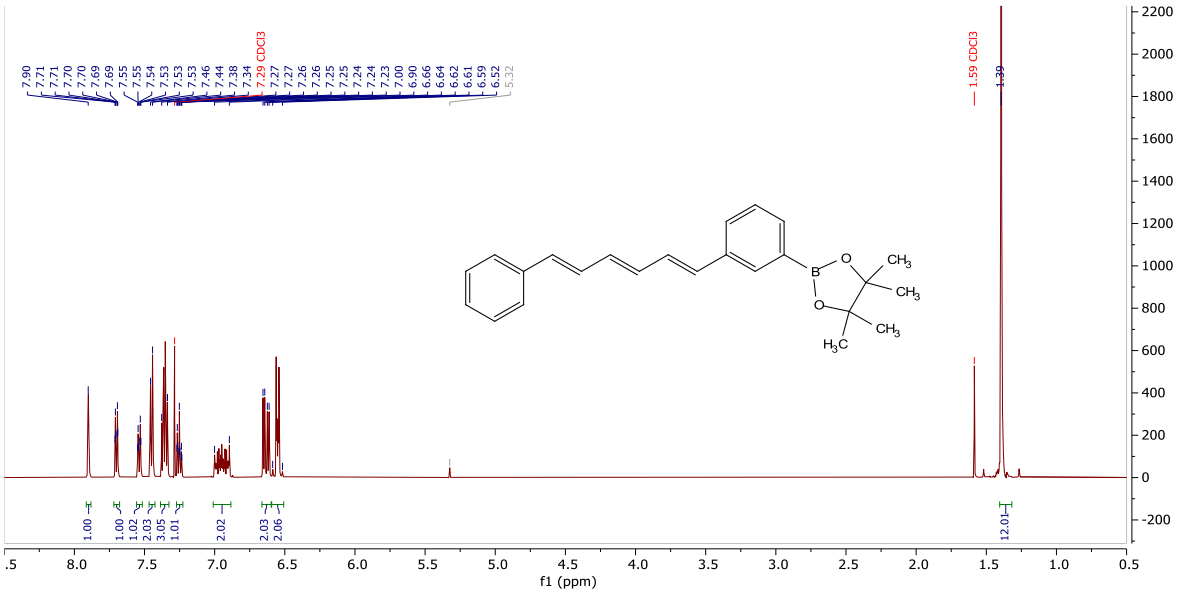

^{13}C NMR, 126 MHz, $CDCl_3$

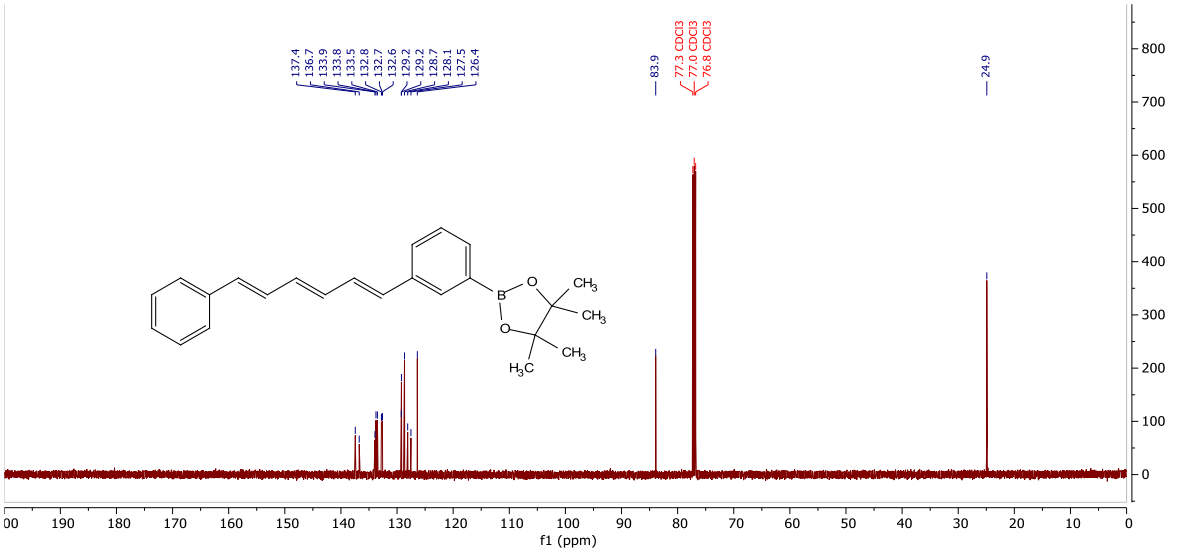

tetraethyl but-2-ene-1,4-diyl(E)-bis(phosphonate) [11]

^{1}H NMR, 500 MHz, $CDCl_3$

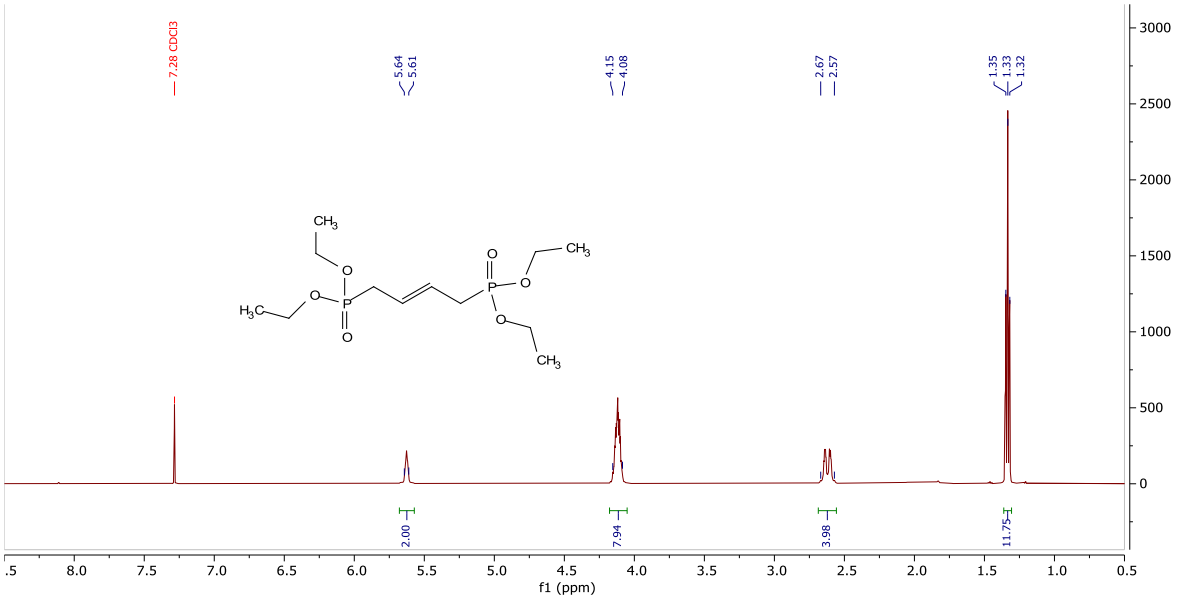

^{13}C NMR, 126 MHz, $CDCl_3$

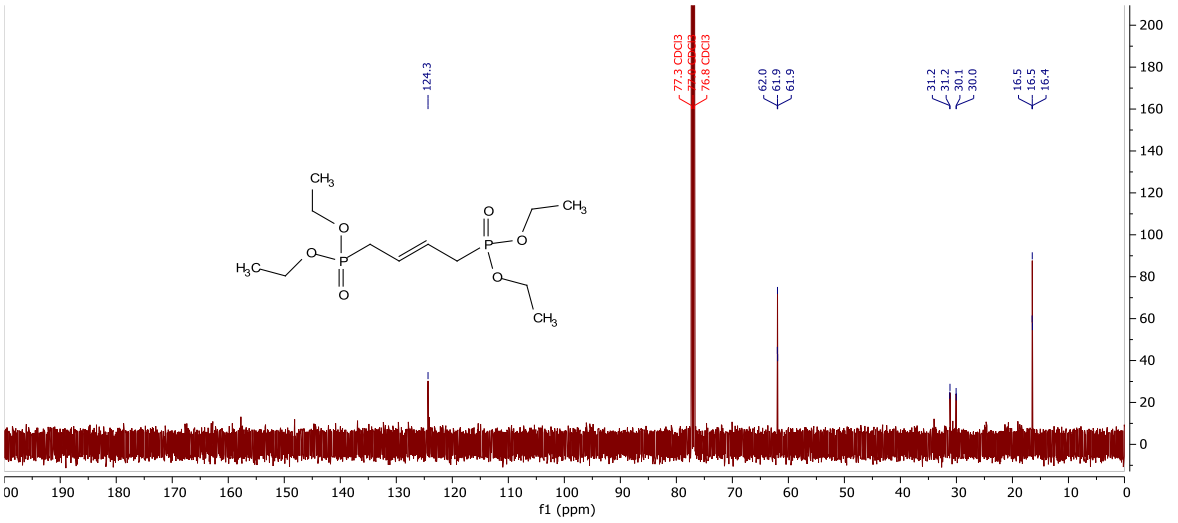

(1E,3E,5E)-1,6-bis(3-bromophenyl)hexa-1,3,5-triene [12]

^{1}H NMR, 500 MHz, $CDCl_3$

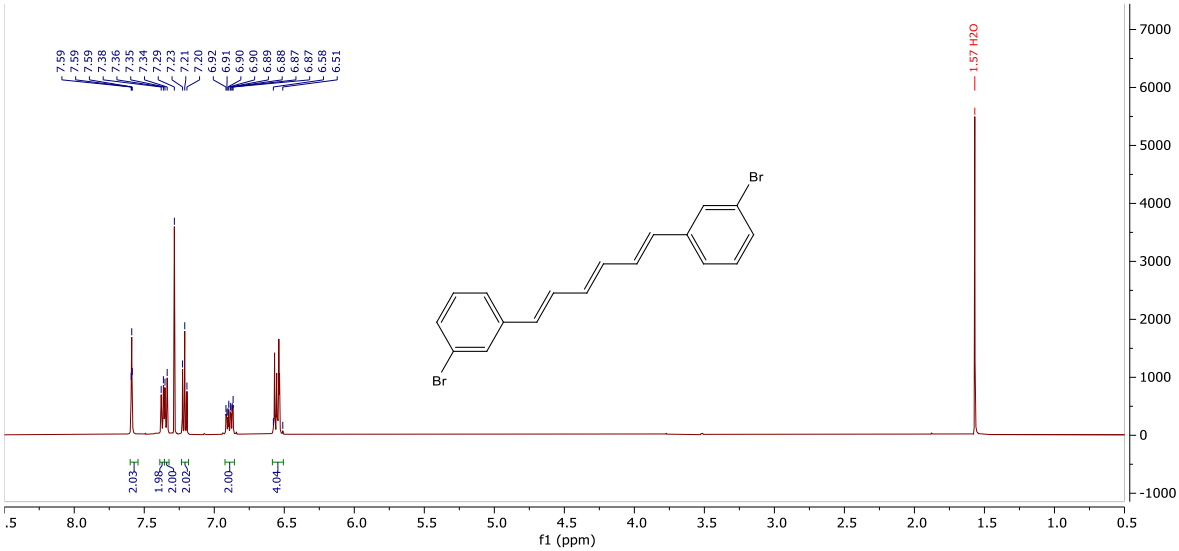

^{13}C NMR, 126 MHz, $CDCl_3$

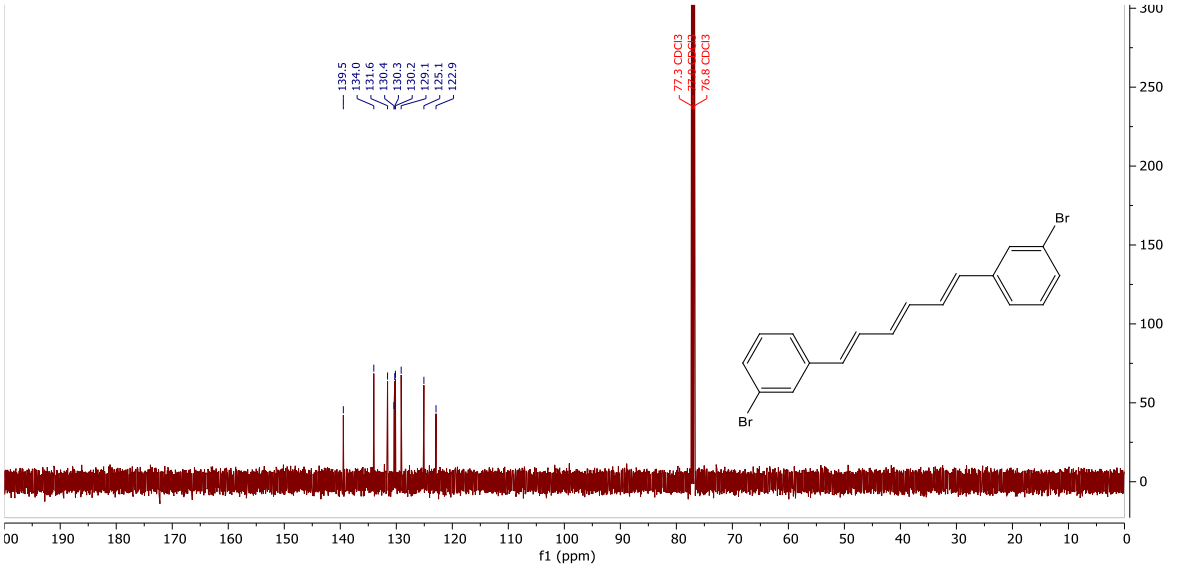

(1E,3E,5E)-1,6-bis(3-(4,4,5,5-tetramethyl-1,3,2-dioxaborolan-2-yl)phenyl)hexa-1,3,5-triene [13]

^{1}H NMR, 500 MHz, $CDCl_3$

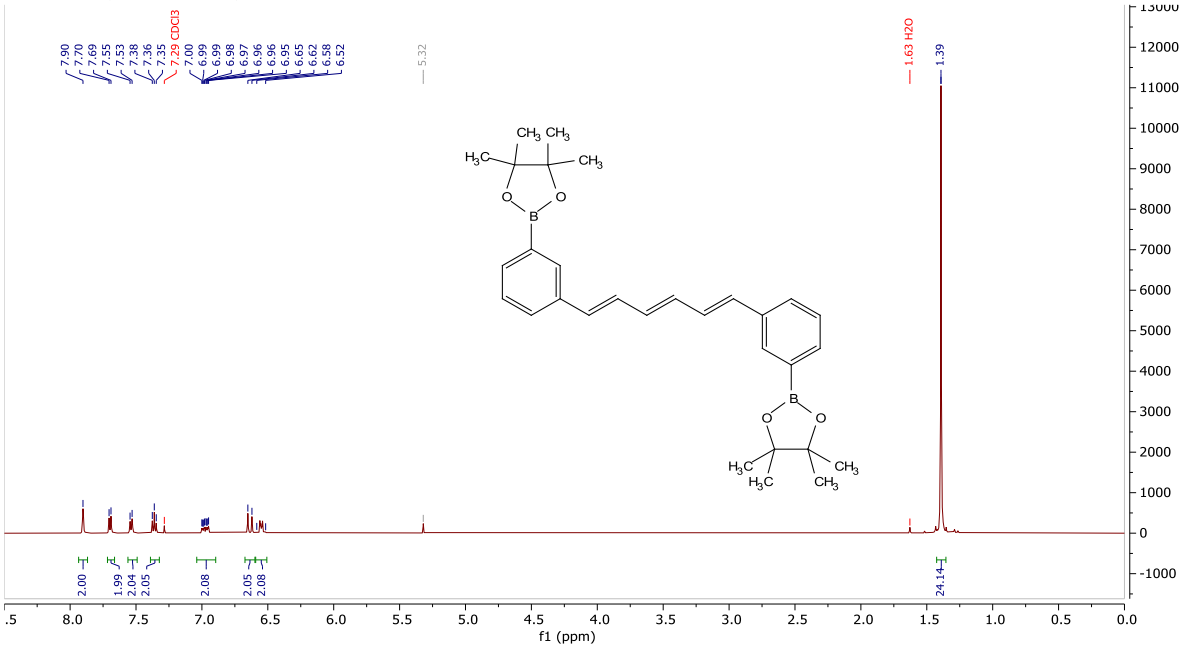

^{13}C NMR, 126 MHz, $CDCl_3$

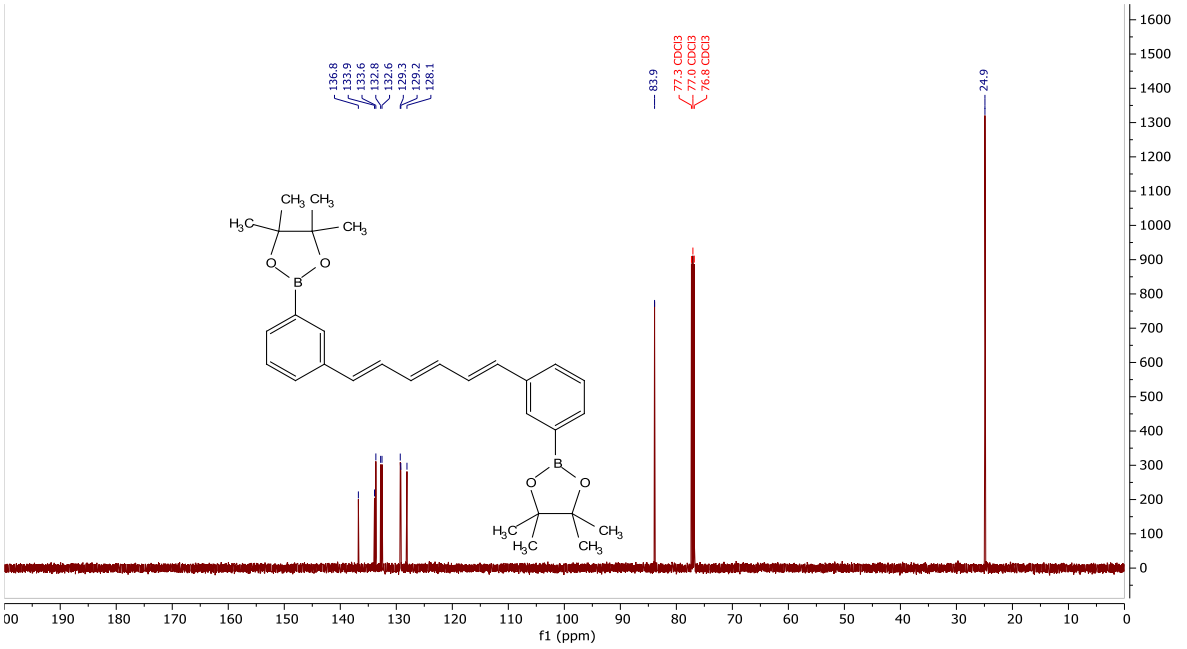

4',5'-bis((2-butyloctyl)oxy)-3,3''-bis((1E,3E,5E)-6-phenylhexa-1,3,5-trien-1-yl)-1,1':2',1''-terphenyl [$(DPH)_2$]

^{1}H NMR, 500 MHz, $CDCl_3$

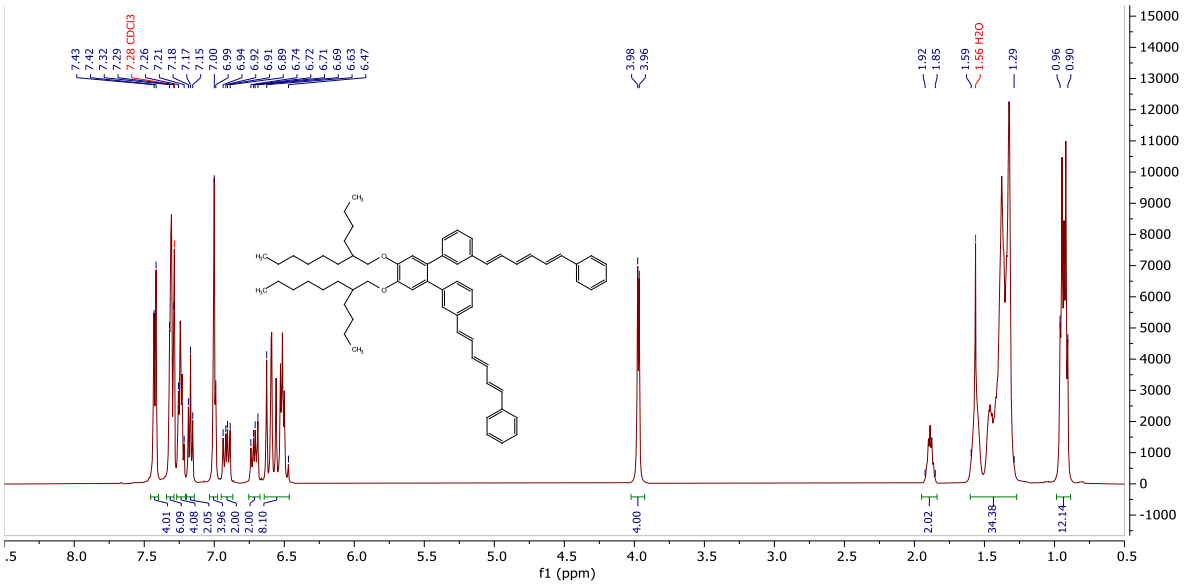

^{13}C NMR, 126 MHz, $CDCl_3$

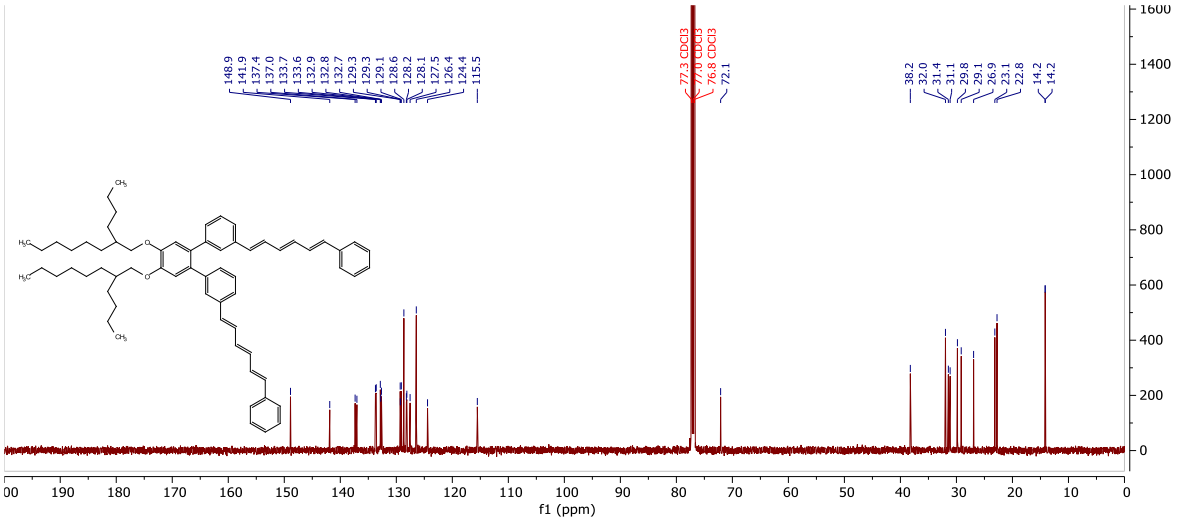

2-bromo-4,5-bis((2-butyloctyl)oxy)-3'-((1E,3E,5E)-6-phenylhexa-1,3,5-trien-1-yl)-1,1'-biphenyl [14]

^{1}H NMR, 500 MHz, $CDCl_3$

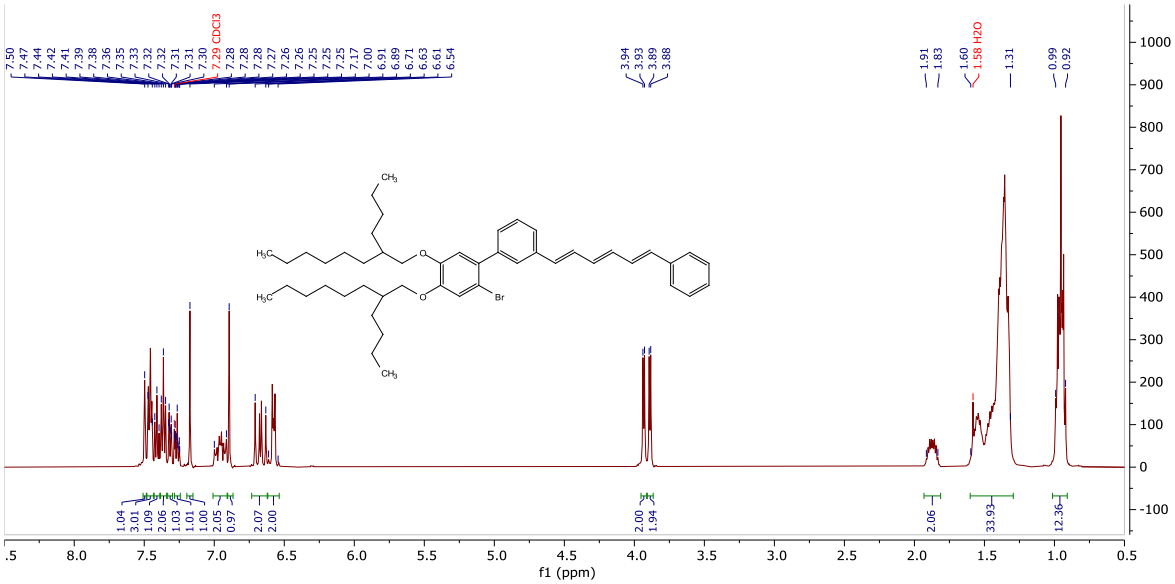

^{13}C NMR, 126 MHz, $CDCl_3$

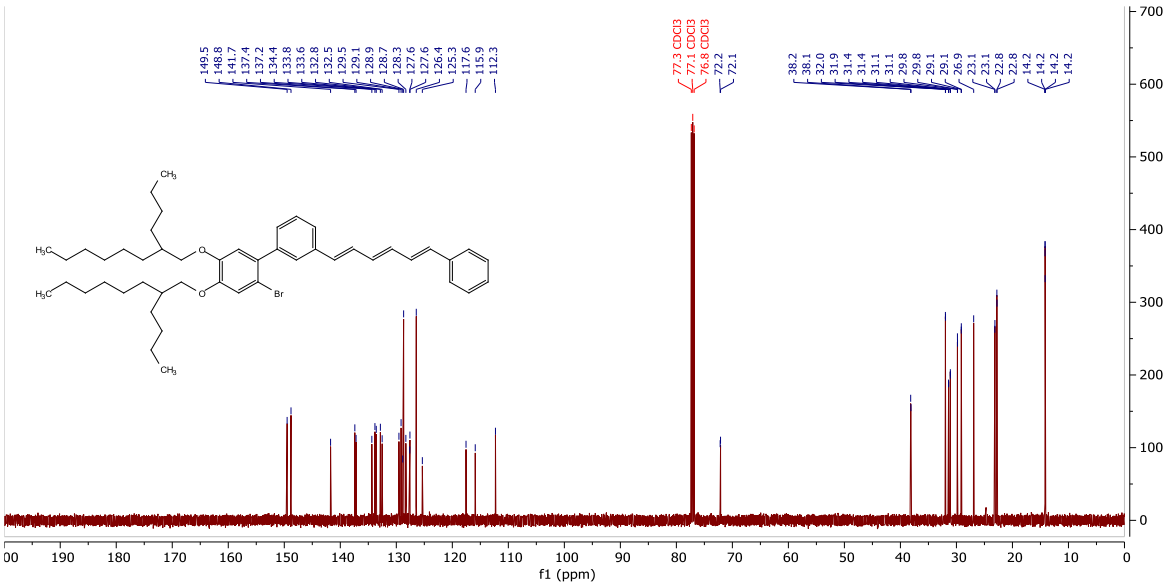

(1E,3E,5E)-1,6-bis(4',5'-bis((2-butyloctyl)oxy)-3''-((1E,3E,5E)-6-phenylhexa-1,3,5-trien-1-yl)-[1,1':2',1''-terphenyl]-3-yl)hexa-1,3,5-triene [$(DPH)_3$]

^{1}H NMR, 500 MHz, $CDCl_3$

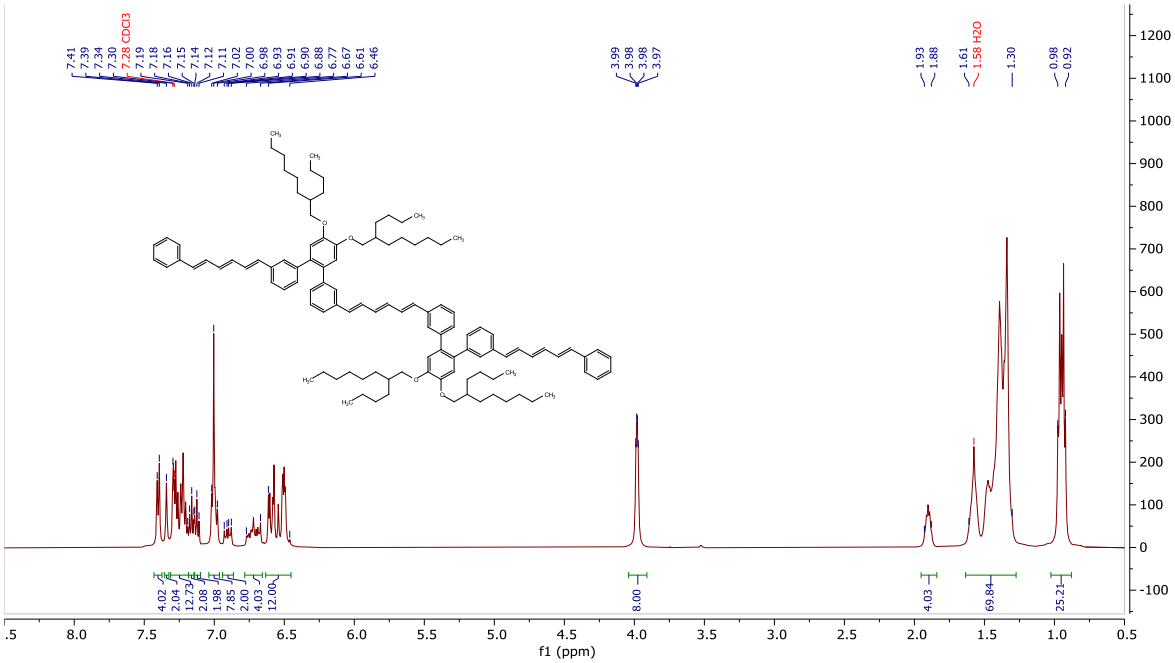

^{13}C NMR, 126 MHz, $CDCl_3$

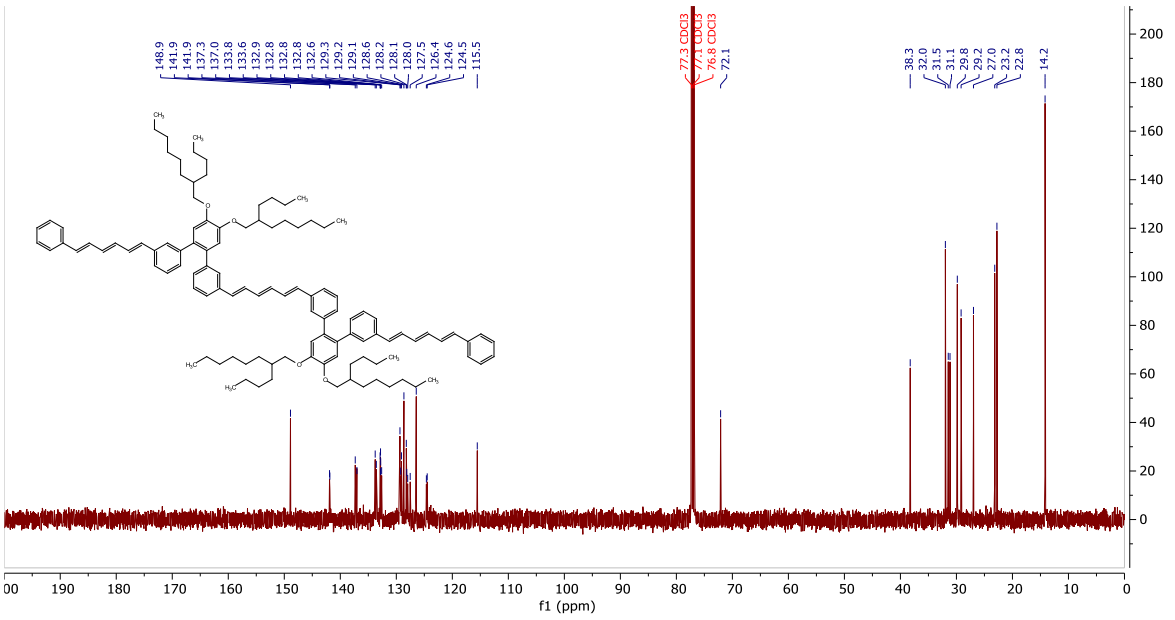

2-(3-((1E,3E,5E)-6-(4',5'-bis((2-butyloctyl)oxy)-3''-((1E,3E,5E)-6-phenylhexa-1,3,5-trien-1-yl)-[1,1':2',1''-terphenyl]-3-yl)hexa-1,3,5-trien-1-yl)phenyl)-4,4,5,5-tetramethyl-1,3,2-dioxaborolane [15]

^{1}H NMR, 500 MHz, $CDCl_3$

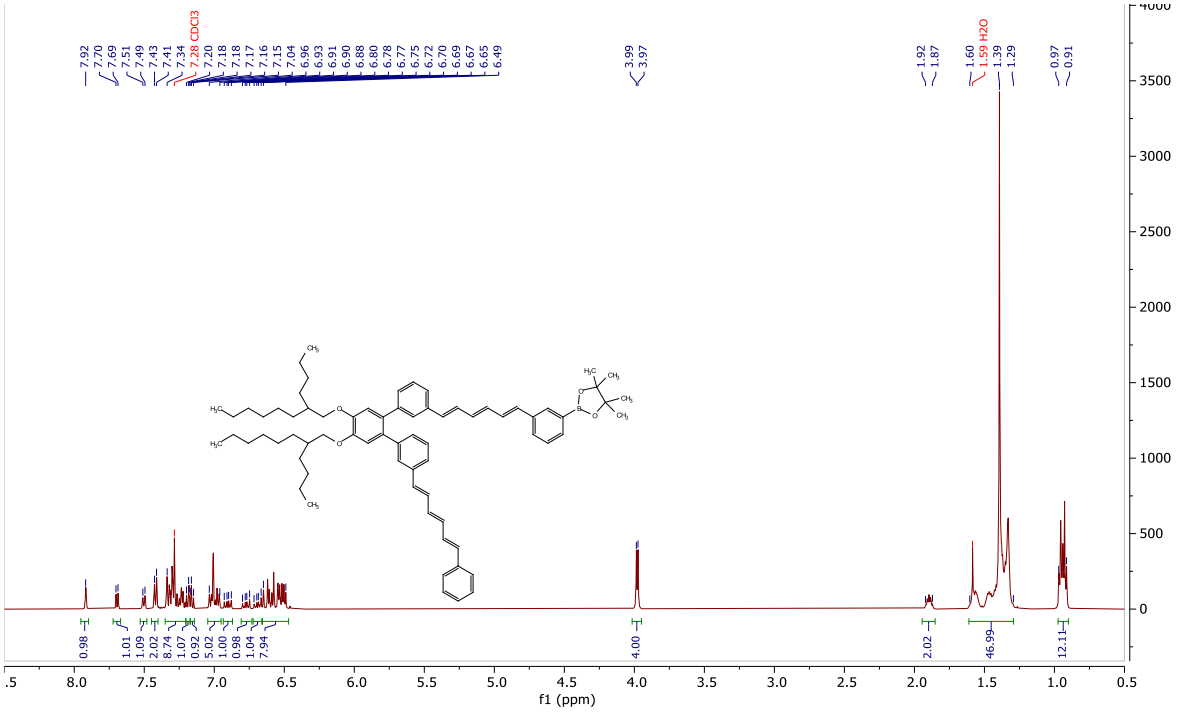

^{13}C NMR, 126 MHz, $CDCl_3$

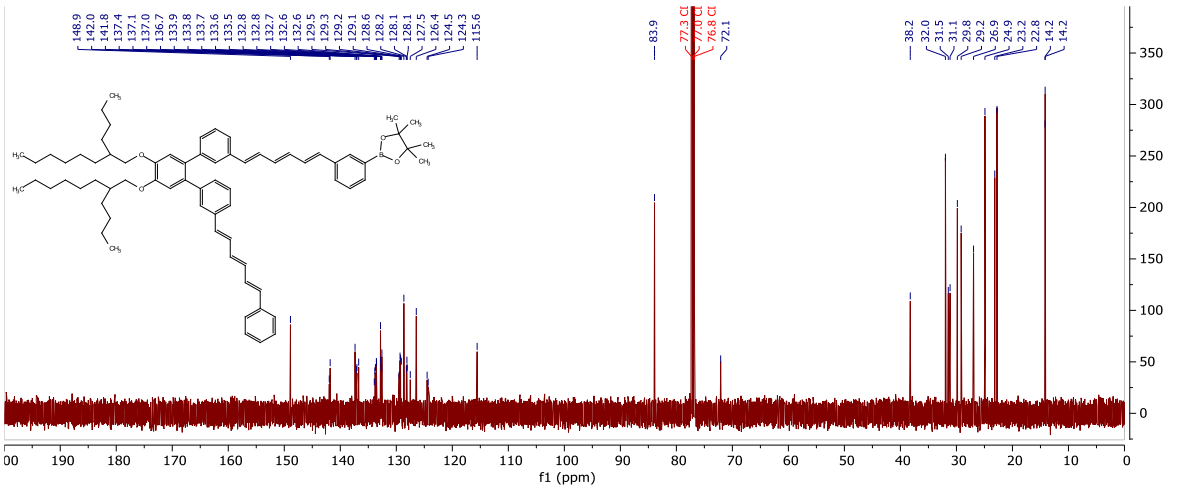

3'',3'''''-((1E,1'E,3E,3'E,5E,5'E)-(4',5'-bis((2-butyloctyl)oxy)-[1,1':2',1''-terphenyl]-3,3''-diyl)bis(hexa-1,3,5-triene-6,1-diyl))bis(4',5'-bis((2-butyloctyl)oxy)-3-((1E,3E,5E)-6-phenylhexa-1,3,5-trien-1-yl)-1''',1'''':2'''',1'''''-terphenyl) [(DPH)$_4$]

^{1}H NMR, 500 MHz, $CDCl_3$

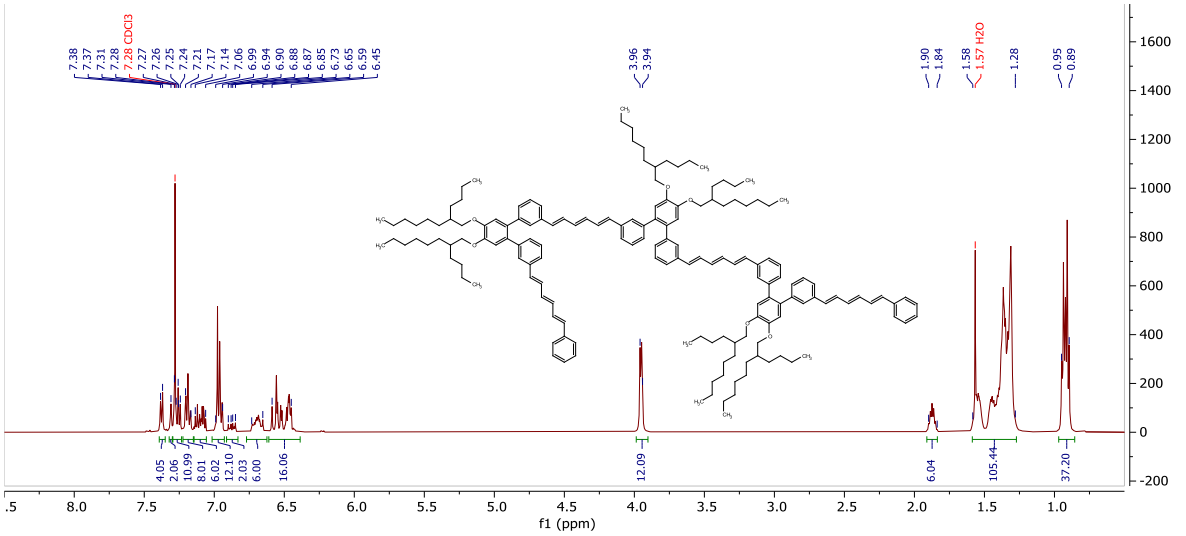

^{13}C NMR, 126 MHz, $CDCl_3$

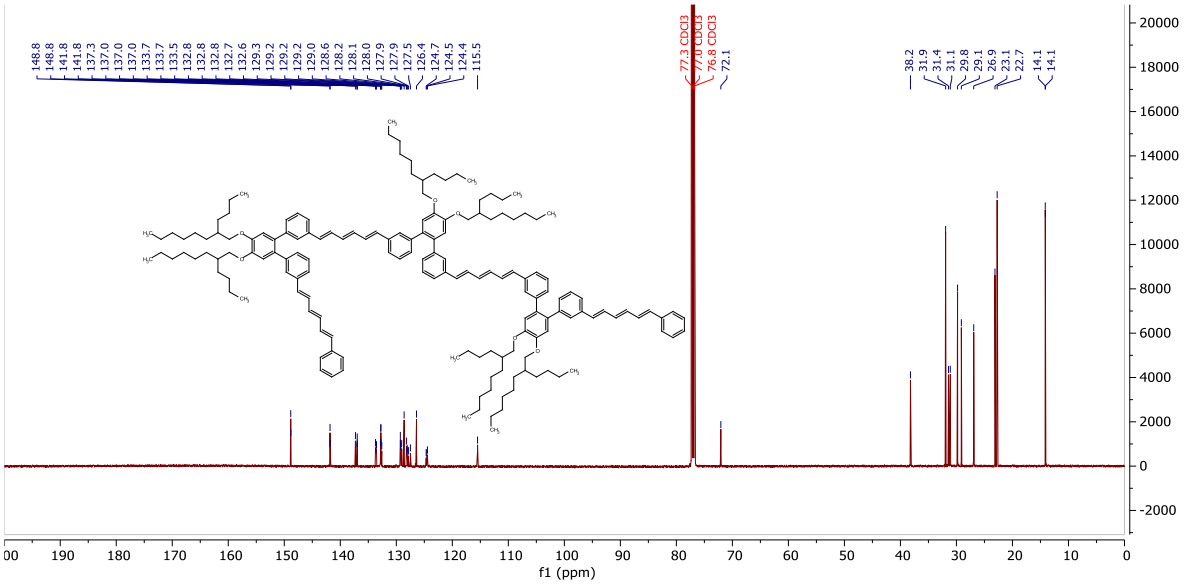

8. Mass Spectra of Oligomers

4',5'-bis((2-butyloctyl)oxy)-3,3''-bis((1E,3E,5E)-6-phenylhexa-1,3,5-trien-1-yl)-1,1':2',1''-terphenyl [(DPH)$_2$]

Elemental Composition Report **Page 1**

Single Mass Analysis
Tolerance = 5.0 PPM / DBE: min = -1.5, max = 50.0
Element prediction: Off
Number of isotope peaks used for i-FIT = 3

Monoisotopic Mass, Even Electron Ions
1 formula(e) evaluated with 1 results within limits (up to 50 best isotopic matches for each mass)
Elements Used:
C: 0-66 H: 0-84 O: 0-2

HAB-O MILLINGTON_OM-2-32 bis
HAB-O MILLINGTON_OM-2-32 bis 689 (1.507) Cm (574:714)

1: TOF MS ASAP+
7.01e+002

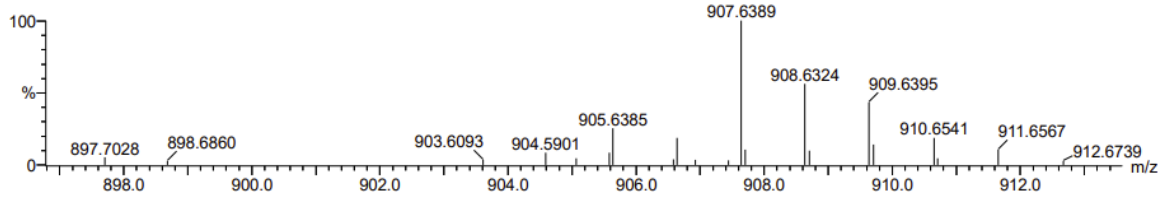

Minimum:				-1.5				
Maximum:		5.0	5.0	50.0				
Mass	Calc. Mass	mDa	PPM	DBE	i-FIT	Norm	Conf(%)	Formula
907.6389	907.6393	-0.4	-0.4	25.5	45.2	n/a	n/a	C66 H83 O2

(1E,3E,5E)-1,6-bis(4',5'-bis((2-butyloctyl)oxy)-3''-((1E,3E,5E)-6-phenylhexa-1,3,5-trien-1-yl)-[1,1':2',1''-terphenyl]-3-yl)hexa-1,3,5-triene [(DPH)$_3$]

Elemental Composition Report **Page 1**

Single Mass Analysis
Tolerance = 1000.0 PPM / DBE: min = -1.5, max = 50.0
Element prediction: Off
Number of isotope peaks used for i-FIT = 3

Monoisotopic Mass, Even Electron Ions
1 formula(e) evaluated with 1 results within limits (up to 50 closest results for each mass)
Elements Used:
C: 1-114 H: 1-150 O: 0-4

SVL_O MILLINGTON_OM-2-38 95 (0.237)

1: TOF MS ES+
1.49e+003

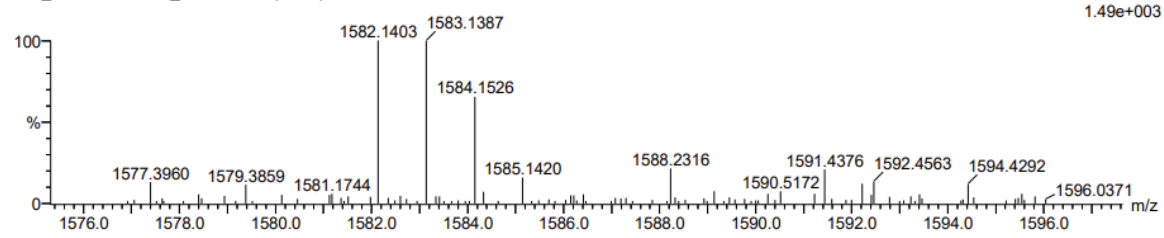

Minimum:				-1.5				
Maximum:		5.0	1000.0	50.0				
Mass	Calc. Mass	mDa	PPM	DBE	i-FIT	Norm	Conf(%)	Formula
1582.1403	1582.1456	-5.3	-3.3	40.5	115.6	n/a	n/a	C114 H149 O4

3'',3''''-((1E,1'E,3E,3'E,5E,5'E)-(4',5'-bis((2-butyloctyl)oxy)-[1,1':2',1''-terphenyl]-3,3''-diyl)bis(hexa-1,3,5-triene-6,1-diyl))bis(4',5'-bis((2-butyloctyl)oxy)-3-((1E,3E,5E)-6-phenylhexa-1,3,5-trien-1-yl)-1''',1'''':2'''',1''''-terphenyl) [(DPH)$_4$]

Elemental Composition Report **Page 1**

Single Mass Analysis
Tolerance = 2000.0 PPM / DBE: min = -1.5, max = 50.0
Element prediction: Off
Number of isotope peaks used for i-FIT = 3

Monoisotopic Mass, Odd and Even Electron Ions
1 formula(e) evaluated with 0 results within limits (up to 50 closest results for each mass)
Elements Used:
C: 0-162 H: 0-217 O: 0-6
OM SAMPLE
OM SAMPLE 353 (6.875) Cm (348:360)

1: TOF MS ES+
6.49e+003

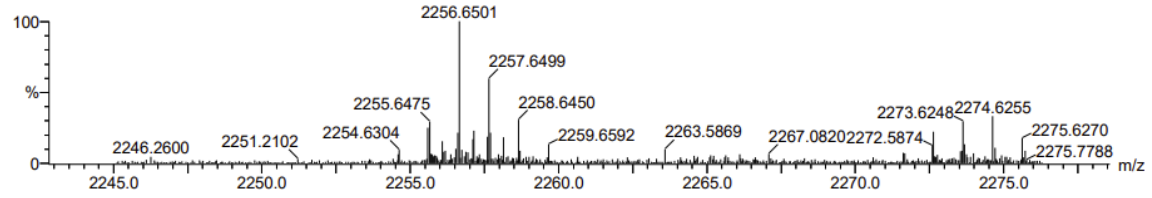


```
Minimum:                          -1.5
Maximum:              5.0    2000.0 50.0

Mass       Calc. Mass  mDa    PPM    DBE    i-FIT   Norm   Conf(%) Formula

2255.6475  ---
```

MALDI

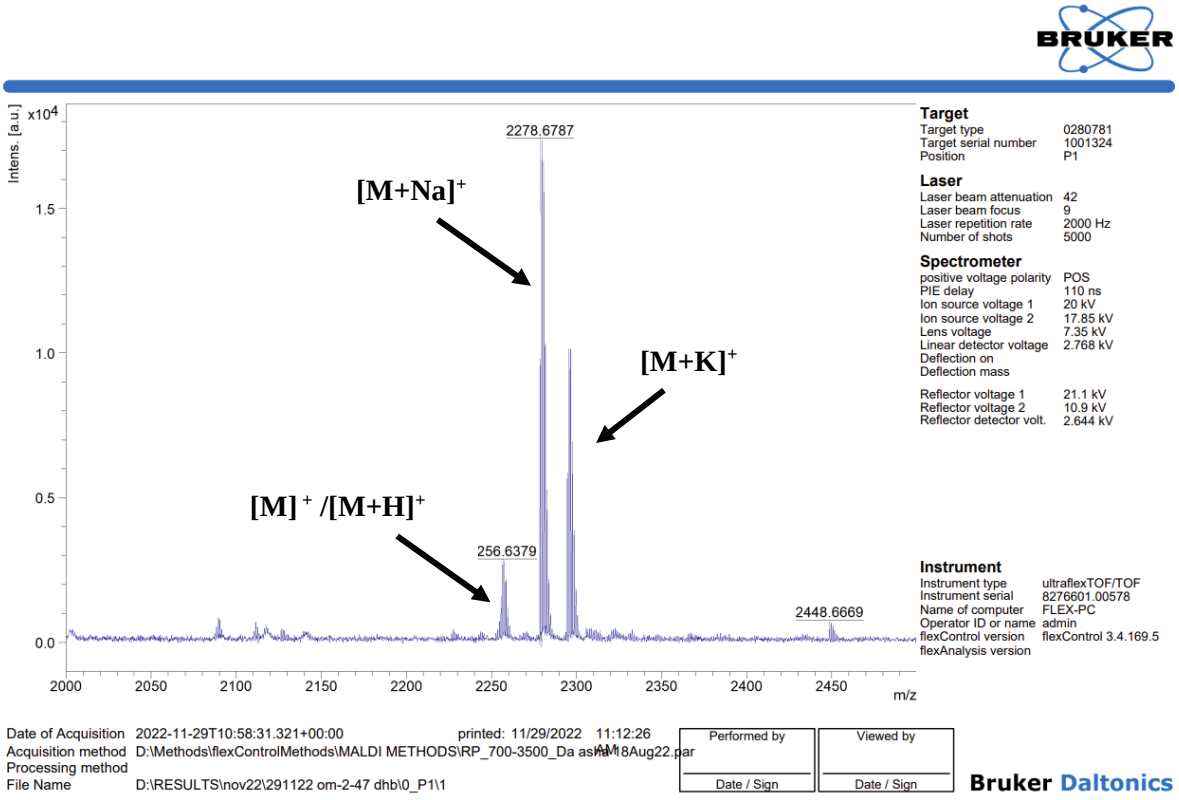

9. References

(1) Millington, O.; Montanaro, S.; Leventis, A.; Sharma, A.; Dowland, S. A.; Sawhney, N.; Fallon, K. J.; Zeng, W.; Congrave, D. G.; Musser, A. J.; Rao, A.; Bronstein, H. Soluble Diphenylhexatriene Dimers for Intramolecular Singlet Fission with High Triplet Energy. *J Am Chem Soc* **2023**. https://doi.org/10.1021/jacs.2c12060.

(2) Brown, R. XXVII. *A Brief Account of Microscopical Observations Made in the Months of June, July and August* 1827, *on the Particles Contained in the Pollen of Plants; and on the General Existence of Active Molecules in Organic and Inorganic Bodies*. *The Philosophical Magazine* **1828**, *4* (21), 161–173. https://doi.org/10.1080/14786442808674769.

(3) Smoluchowski, M. v. Versuch Einer Mathematischen Theorie Der Koagulationskinetik Kolloider Lösungen. *Zeitschrift für Physikalische Chemie* **1918**, *92U* (1), 129–168. https://doi.org/10.1515/zpch-1918-9209.

(4) Berg, O. G.; von Hippel, P. H. Diffusion-Controlled Macromolecular Interactions. *Annu Rev Biophys Biophys Chem* **1985**, *14* (1), 131–158. https://doi.org/10.1146/annurev.bb.14.060185.001023.

(5) Harada, J.; Harakawa, M.; Ogawa, K. Conformational Change of All-Trans-1,6-Diphenyl-1,3,5-Hexatriene in Two Crystalline Forms. *CrystEngComm* **2008**, *10* (12), 1777. https://doi.org/10.1039/b811220g.

(6) Frisch, M. J.; Trucks, G. W.; Schlegel, H. B.; Scuseria, G. E.; Robb, M. A.; Cheeseman, J. R.; Scalmani, G.; Barone, V.; Petersson, G. A.; Nakatsuji, H.; Li, X.; Caricato, M.; Marenich, A. V.; Bloino, J.; Janesko, B. G.; Gomperts, R.; Mennucci, B.; Hratchian, H. P.; Ortiz, J. V.; Izmaylov, A. F.; Sonnenberg, J. L.; Williams-Young, D.; Ding, F.; Lipparini, F.; Egidi, F.; Goings, J.; Peng, B.; Petrone, A.; Henderson, T.; Ranasinghe, D.; Zakrzewski, V. G.; Gao, J.; Rega, N.; Zheng, G.; Liang, W.; Hada, M.; Ehara, M.; Toyota, K.; Fukuda, R.; Hasegawa, J.; Ishida, M.; Nakajima, T.; Honda, Y.; Kitao, O.; Nakai, H.; Vreven, T.; Throssell, K.; Montgomery, J. A. , Jr.; Peralta, J. E.; Ogliaro, F.; Bearpark, M. J.; Heyd, J. J.; Brothers, E. N.; Kudin, K. N.; Staroverov, V. N.; Keith, T. A.; Kobayashi, R.; Normand, J.; Raghavachari, K.; Rendell, A. P.; Burant, J. C.; Iyengar, S. S.; Tomasi, J.; Cossi, M.; Millam, J. M.; Klene, M.; Adamo, C.; Cammi, R.; Ochterski, J. W.; Martin, R. L.; Morokuma, K.; Farkas, O.; Foresman, J. B.; Fox, D. J. Gaussian 16, Revision A.03. Gaussian, Inc.: Wallingford CT 2016.

(7) Zhao, Y.; Truhlar, D. G. The M06 Suite of Density Functionals for Main Group Thermochemistry, Thermochemical Kinetics, Noncovalent Interactions, Excited States, and Transition Elements: Two New Functionals and Systematic Testing of Four M06-Class

Functionals and 12 Other Function. *Theor Chem Acc* **2008**, *120* (1–3), 215–241. https://doi.org/10.1007/s00214-007-0310-x.

(8) Zheng, J.; Xu, X.; Truhlar, D. G. Minimally Augmented Karlsruhe Basis Sets. *Theor Chem Acc* **2011**, *128* (3), 295–305. https://doi.org/10.1007/s00214-010-0846-z.

(9) He, G.; Parenti, K. R.; Campos, L. M.; Sfeir, M. Y. Direct Exciton Harvesting from a Bound Triplet Pair. *Advanced Materials* **2022**, *34* (40), 2203974. https://doi.org/10.1002/adma.202203974.

(10) Evans, R.; Dal Poggetto, G.; Nilsson, M.; Morris, G. A. Improving the Interpretation of Small Molecule Diffusion Coefficients. *Anal Chem* **2018**, *90* (6), 3987–3994. https://doi.org/10.1021/acs.analchem.7b05032.

(11) Walker, B. J.; Musser, A. J.; Beljonne, D.; Friend, R. H. Singlet Exciton Fission in Solution. *Nat Chem* **2013**, *5* (12), 1019–1024. https://doi.org/10.1038/nchem.1801.

(12) Stern, H. L.; Musser, A. J.; Gelinas, S.; Parkinson, P.; Herz, L. M.; Bruzek, M. J.; Anthony, J.; Friend, R. H.; Walker, B. J. Identification of a Triplet Pair Intermediate in Singlet Exciton Fission in Solution. *Proceedings of the National Academy of Sciences* **2015**, *112* (25), 7656–7661. https://doi.org/10.1073/pnas.1503471112.

(13) Jökel, J.; Schwer, F.; von Delius, M.; Apfel, U.-P. A Dinuclear Porphyrin-Macrocycle as Efficient Catalyst for the Hydrogen Evolution Reaction. *Chemical Communications* **2020**, *56* (91), 14179–14182. https://doi.org/10.1039/D0CC05229A.

(14) Leung, A. C. W.; MacLachlan, M. J. Poly(Salphenyleneethynylene)s: Soluble, Conjugated Metallopolymers That Exhibit Unique Supramolecular Crosslinking Behavior. *J Mater Chem* **2007**, *17* (19), 1923. https://doi.org/10.1039/b618833h.

(15) Chen, Z.-K.; Lee, N. H. S.; Huang, W.; Xu, Y.-S.; Cao, Y. New Phenyl-Substituted PPV Derivatives for Polymer Light-Emitting Diodes−Synthesis, Characterization and Structure−Property Relationship Study. *Macromolecules* **2003**, *36* (4), 1009–1020. https://doi.org/10.1021/ma021221n.

(16) Motika, S. E.; Wang, Q.; Ye, X.; Shi, X. Ambient Synthesis of Dienals via Triazole–Gold and Amine Catalysis Relay. *Org Lett* **2015**, *17* (2), 290–293. https://doi.org/10.1021/ol503393a.

(17) Vaz, B.; Fontán, N.; Castiñeira, M.; Álvarez, R.; de Lera, Á. R. Synthesis of Labile All-Trans-7,8,7′,8′-Bis-Acetylenic Carotenoids by Bi-Directional Horner–Wadsworth–Emmons Condensation. *Org Biomol Chem* **2015**, *13* (10), 3024–3031. https://doi.org/10.1039/C4OB02144D.